# Adaptive Reduced-Rank Minimum Symbol-Error-Rate Receive Processing for Large-Scale Multiple-Antenna Systems

Yunlong Cai, Rodrigo C. de Lamare, Benoit Champagne, Boya Qin, and Minjian Zhao

arXiv:1510.07735v1 [cs.IT] 27 Oct 2015

***Abstract*—In this work, we propose a novel adaptive reduced-rank receive processing strategy based on joint preprocessing, decimation and filtering (JPDF) for large-scale multiple-antenna systems. In this scheme, a reduced-rank framework is employed for linear receive processing and multiuser interference suppression based on the minimization of the symbol-error-rate (SER) cost function. We present a structure with multiple processing branches that performs a dimensionality reduction, where each branch contains a group of jointly optimized preprocessing and decimation units, followed by a linear receive filter. We then develop stochastic gradient (SG) algorithms to compute the parameters of the preprocessing and receive filters, along with a low-complexity decimation technique for both binary phase shift keying (BPSK) and $M$-ary quadrature amplitude modulation (QAM) symbols. In addition, an automatic parameter selection scheme is proposed to further improve the convergence performance of the proposed reduced-rank algorithms. Simulation results are presented for time-varying wireless environments and show that the proposed JPDF minimum-SER receive processing strategy and algorithms achieve a superior performance than existing methods with a reduced computational complexity.**

***Index Terms*—Adaptive algorithms, minimum-SER, reduced-rank techniques, large-scale multiple-antenna systems.**

## I. Introduction

The use of large-scale multiple-antenna systems, as in e.g., massive multiple-input multiple-output (MIMO) communications, has become a highly popular approach to support the efficient and flexible multiple access schemes needed in the next generation of wireless cellular, local area [1]-[6] and multibeam satellite networks [5]. In this context, a key problem that has been receiving significant attention is the design of efficient and flexible space-time processing techniques at the receiver side. Space-time processing can be used to separate signals transmitted in the same frequency band, and provides a practical means of supporting multiple users through space division multiple access [7]-[9]. Indeed, systems equipped with large-scale antenna arrays can substantially increase the system capacity and improve the quality and reliability of wireless links via beamforming and spatial multiplexing [10]. The problem of detecting a desired user's signal in a multiuser large-scale multiple-antenna system presents many signal processing challenges, including: the need for algorithms with the ability to process large-dimensional received data vectors, fast and accurate adjustment of system parameters, scalable computational complexity and the development of cost-effective interference mitigation schemes.

Adaptive techniques are among the most commonly used approaches to continually adjust the receiver weights for detecting a desired signal, while coping with changes in the radio signal environment and reducing computational complexity [11]. However, one problem for the standard, i.e. full-rank adaptive algorithms is that their convergence performance deteriorates rapidly with an increase in the eigenvalue spread of the received data covariance matrix, as measured by its condition number [12]-[15].[1] This situation is usually worse when a filter with a large number of adaptive weights is employed to operate on large-dimensional received data vectors. In this context, reduced-rank signal processing has received significant attention in the past years and it has become a key technique for application to large adaptive systems, since it can provide faster training, better tracking performance and increased robustness against interference as compared to standard methods. The reduced-rank technique projects the large-dimensional received data vector onto a lower dimensional subspace and performs the filtering optimization within this subspace. A number of reduced-rank algorithms have been developed to design the subspace projection matrix and the reduced-rank receive filter [12]-[30]. Among the first schemes are the eigendecomposition-based (EIG) algorithms [12], [13] and the multistage Wiener filter (MSWF) investigated in [14], [15]. EIG and MSWF have fast convergence speed, but their computational complexity is relatively high. A strategy based on the joint and iterative optimization (JIO) of a subspace projection matrix and a reduced-rank receive filter has been reported in [21]-[26], whereas algorithms using joint prepro-

Y. Cai, B. Qin and M. Zhao are with Department of Information Science and Electronic Engineering, Zhejiang University, Hangzhou 310027, China (e-mail: ylcai@zju.edu.cn; qby666@zju.edu.cn; mjzhao@zju.edu.cn).

R. C. de Lamare is with CETUC-PUC-Rio, 22453-900 Rio de Janeiro, Brazil, and also with the Communications Research Group, Department of Electronics, University of York, YO10 5DD York, U.K. (e-mail: rcdl500@ohm.york.ac.uk).

B. Champagne is with the Department of Electrical and Computer Engineering, McGill University, Montreal, QC, Canada, H3A 0E9 (e-mail: benoit.champagne@mcgill.ca).

This work was supported in part by the National Natural Science Foundation of China under Grant 61471319, Zhejiang Provincial Natural Science Foundation of China under Grant LY14F010013, the Fundamental Research Funds for the Central Universities, and the National High Technology Research and Development Program (863 Program) of China under Grant 2014AA01A707.

[1] In the current context of multi-user transceiver design, reduced-rank techniques were primarily meant to reduce the complexity of non-adaptive full-rank algorithms [16] and increase the speed of adaptive parameter estimation tasks. While the computational complexity of on-line full-rank adaptive algorithms such as stochastic gradient (SG) based algorithms (e.g., least-mean square (LMS) and its variations) is relatively small, they are characterized by extremely slow convergence in these applications, as will be illustrated in Section VI. The main problem of interest, therefore, is how to design low-complexity reduced-rank algorithms to increase the convergence speed and tracking performance in the presence of large-dimensional filters.

cessing, decimation and filtering (JPDF) schemes have been considered in [27]-[32].

However, most of the contributions to date are either based on the minimization of the mean square error (MSE) and/or the minimum variance criteria [11]-[32], which are not the most appropriate metrics from a performance viewpoint in digital communications where a standard measure of transmission reliability is the symbol-error-rate (SER) rather than MSE. Transceiver design approaches that can minimize the SER have been reported in [7], [33]-[39] and are termed adaptive minimum-SER (MSER) techniques. It is also well known that MSER algorithms lose their advantage when working with large filters and that the use of reduced-rank techniques can speed up their training. The work in [38] appears to be the first approach to devise a reduced-rank algorithm with the MSER criterion. However, the resulting scheme is a hybrid between an EIG or an MSWF approach, and a SER scheme in which only the reduced-rank receive filter is adjusted in an MSER fashion. The recently reported work in [40] investigates a novel adaptive reduced-rank strategy based on JIO of the receive filters according to the MSER criterion. The performance results verify that the MSER-JIO reduced-rank algorithm outperforms the MSER-EIG and the MSER-MSWF reduced-rank algorithms. A limitation of the work in [40] is that the subspace projection matrix might contain a very large number of parameters in large-scale multiple-antenna systems, which increases the cost and impacts the training of the receiver. To the best of our knowledge, these existing works on MSER techniques have not addressed the key problem of performance degradation experienced when the filters become larger and their convergence is slow compared to that of MSE-based techniques.

In this work, we propose a new adaptive reduced-rank receive processing front-end for multiuser large-scale multiple-antenna systems that incorporates the joint preprocessing, decimation and filtering (JPDF) structure adaptively optimized on the basis of the MSER criterion. The proposed scheme employs a multiple-branch structural framework, where each branch contains a preprocessing filter, a decimation unit and a linear reduced-rank receive filter. It constitutes a general receive front-end which can be combined with several linear and nonlinear receiver architecture, but with the key advantage of requiring a much smaller set of adaptive parameters for its adjustment. The dimensionality reduction is carried out by the preprocessing filter and the decimation unit. After dimensionality reduction, a linear receive filter with reduced dimensionality is applied to suppress the multiuser interference and provide an estimate of the desired user's symbols. The final decision is generated among the branch estimates according to the minimum Euclidean distance between a training symbol and the output of each filtering branch. At each time instant, the preprocessing filter and the reduced-rank receive filter are optimized based on the MSER criterion using the given decimation unit for each branch. We devise stochastic gradient (SG) algorithms to compute the parameters of the preprocessing and receive filters along with a low-complexity decimation technique for both binary phase shift keying (BPSK) symbols and $M$-ary quadrature amplitude modulation (QAM) symbols. A unique feature of our scheme is that all component filters have a small number of parameters and yet can ensure the effectiveness of MSER-type methods. In order to further improve the convergence performance of the proposed algorithms, we also develop an automatic parameter selection scheme to determine the lengths of the preprocessor and the reduced-rank receive filter.

The proposed reduced-rank MSER-JPDF technique can operate as a receive-processing front-end which is much simpler than a zero forcing (ZF) or minimum mean square error (MMSE) filter. It can be combined with other interference cancellation algorithms and offers a significantly better performance than the matched filter. A detailed analysis of the SG-based adaptive MSER algorithm for updating the parameters of the reduced-rank JPDF structure is carried out in terms of computational complexity and convergence behavior. In simulations over multipath time-varying fading channels, the proposed MSER-JPDF receive processing strategy and adaptive algorithms exhibit a performance much superior to that of full-rank adaptive techniques. Furthermore, compared to existing MSER-based reduced-rank algorithms, the new algorithms can significantly reduce the computational complexity and speed up the training. The contributions of this paper are summarized as follows:

I) A novel MSER reduced-rank scheme that incorporates the JPDF structure is proposed for multiuser large-scale multiple-antenna systems.
II) For each branch of the JPDF structure, we develop adaptive SG algorithms to update the preprocessing and receive filters for BPSK and QAM symbols according to the MSER criterion.
III) We also propose a selection mechanism for choosing the optimal branch corresponding to the minimum Euclidean distance and present a low-complexity design for the decimation unit.
IV) An automatic parameter selection scheme is proposed to further increase the convergence performance of the proposed reduced-rank algorithms.
V) For the proposed algorithms, we perform a detailed performance analysis in terms of computational complexity and convergence.

The paper is structured as follows. Section II briefly describes the system model and the problem statement, while the JPDF reduced-rank scheme is introduced in Section III. In Section IV, the proposed adaptive MSER-JPDF reduced-rank algorithms are developed to efficiently update the preprocessing filter and the reduced-rank receive filter for both BPSK and QAM symbols. The analysis of computational complexity and convergence behavior for the proposed algorithms is conducted in Section V. The simulation results are presented in Section VI while conclusions are drawn in Section VII.

## II. System Model and Problem Statement

We consider the uplink of a large-scale multiple-antenna system with $K$ mobile users and a base station comprised of $L$ identical omnidirectional antenna elements, where $L$ is a large integer and $K \ll L$. The signals from the $K$ users are modulated and transmitted over multipath channels, after which they are received and demodulated by the base station. In this work, the propagation effects of the multipath channels

$$\mathbf{H}_{\nu,k}(i) = \begin{pmatrix} h_{k,\nu,0}(i) & \cdots & h_{k,\nu,L_p-1}(i) & & \\ & h_{k,\nu,0}(i-1) & \cdots & h_{k,\nu,L_p-1}(i-1) & \\ & & \ddots & \cdots & \ddots \\ & & & h_{k,\nu,0}(i-P+1) & \cdots \quad h_{k,\nu,L_p-1}(i-P+1) \end{pmatrix} \tag{4}$$

are modeled by finite impulse response (FIR) filters with $L_p$ coefficients. We assume that the channel can vary over a block of transmitted symbols and that the receivers remain perfectly synchronized with the main propagation path.

The demodulated signal received at the $\nu$-th antenna element and $i$-th time instant, after applying a filter matched to the signal waveform and sampling at symbol rate, is expressed by

$$r_\nu(i) = \sum_{k=0}^{K-1} \sum_{\mu=0}^{L_p-1} h_{k,\nu,\mu}(i) b_k(i-\mu) + n_\nu(i), \quad \nu \in \{0,\ldots,L-1\}, \tag{1}$$

where $h_{k,\nu,\mu}(i)$ is the sampled impulse response between user $k$ and receive antenna $\nu$ for path $\mu \in \{0,\ldots,L_p-1\}$, $b_k(i)$ are the data symbols of user $k \in \{0,\ldots,K-1\}$, and $n_\nu(i)$ are samples of white Gaussian noise. By collecting the samples of the received signal and organizing them in a window of $P$ symbols for each antenna element, we obtain the $LP \times 1$ received vector as

$$\mathbf{r}(i) = \mathbf{H}(i)\mathbf{b}(i) + \mathbf{n}(i). \tag{2}$$

In this expression, $\mathbf{r}(i) = [\mathbf{r}_0^T(i),\ldots,\mathbf{r}_{L-1}^T(i)]^T$ contains the signals that are collected by the $L$ antennas, the $P \times 1$ vector $\mathbf{r}_\nu(i) = [r_\nu(i),\ldots,r_\nu(i-P+1)]^T$, contains the signals that are collected by the $\nu$-th antenna and are organized into a vector. The $K(P+L_p-1) \times 1$ vector $\mathbf{b}(i) = [\mathbf{b}_0^T(i),\ldots,\mathbf{b}_{K-1}^T(i)]^T$ is composed of the data symbols that are transmitted from the $K$ users, with $\mathbf{b}_k(i) = [b_k(i),\ldots,b_k(i-(P+L_p-2))]^T$ being the $i$-th block of transmitted symbols with dimensions $(P+L_p-1)\times 1$. The $LP \times K(P+L_p-1)$ channel matrix $\mathbf{H}(i)$ is expressed as

$$\mathbf{H}(i) = \begin{pmatrix} \mathbf{H}_{0,0}(i) & \mathbf{H}_{0,1}(i) & \cdots & \mathbf{H}_{0,K-1}(i) \\ \mathbf{H}_{1,0}(i) & \mathbf{H}_{1,1}(i) & \cdots & \mathbf{H}_{1,K-1}(i) \\ \vdots & \vdots & \ddots & \vdots \\ \mathbf{H}_{L-1,0}(i) & \mathbf{H}_{L-1,1}(i) & \cdots & \mathbf{H}_{L-1,K-1}(i) \end{pmatrix} \tag{3}$$

where the $P \times (P+L_p-1)$ matrices $\mathbf{H}_{\nu,k}(i)$ are given by (4). Specifically, let us assume that the sequence of transmitted symbols by the $k$-th users, i.e., $b_k(i)$, are independent and identically distributed (i.i.d) random variables drawn from a given symbol set. In this work, BPSK and $M$-ary square QAM symbol constellations are adopted, although extensions to other types of constellations are possible. For the BPSK case, the symbols $b_k(i)$ are uniformly drawn from $\{\pm 1\}$. For the $M$-ary square QAM case, the symbols are uniformly drawn from $\{F_m + jF_n : 1 \le m,n \le \sqrt{M}\}$, where integer $M$ is a perfect square and we define $F_n = 2n - \sqrt{M} - 1$. Without loss of generality, we index the desired user as $k=0$. The term $\mathbf{n}(i) \in \mathbb{C}^{LP\times 1}$ is an additive noise vector, which is assumed to be Gaussian, spatially white, independent over time, with zero-mean and covariance matrix $E[\mathbf{n}(i)\mathbf{n}^H(i)] = \sigma^2\mathbf{I}$, where $\sigma^2$ denotes the variance, $\mathbf{I}$ is an identity matrix of dimension $LP$, and $(.)^H$ stands for the Hermitian transpose operation. The transmitted symbols from the different users and the noise vectors are mutually independent.

The full-rank beamforming receiver design is equivalent to determining an FIR filter $\mathbf{w}(i)$ with $LP$ coefficients that provide an estimate of the desired signal as

$$\hat{b}_0(i) = \mathcal{Q}\{\mathbf{w}^H(i)\mathbf{r}(i)\}, \tag{5}$$

where $\mathcal{Q}\{.\}$ represents the quantization operation for the given constellation and $\mathbf{w}(i) = [w_0,\ldots,w_{LP-1}]^T \in \mathbb{C}^{LP\times 1}$ is the complex weight vector of the receive filter. However, the dimensionality of $\mathbf{w}(i)$ can become excessive for large antenna-array systems, which leads to computationally intensive implementations and slow convergence performance when full-rank adaptive algorithms are employed [12]-[15]. The reduced-rank schemes, which process the received vector $\mathbf{r}(i)$ in two stages, have been proposed to overcome these limitations [12]-[26]. The first stage performs a dimensionality reduction by projecting the large dimensional data vector $\mathbf{r}(i)$ onto a lower dimensional subspace. The second stage is carried out by a reduced-rank receive filter. The output of a reduced-rank scheme is given by

$$\hat{b}_0(i) = \mathcal{Q}\{\bar{\mathbf{w}}^H(i)\mathbf{S}_D^H(i)\mathbf{r}(i)\} = \mathcal{Q}\{\bar{\mathbf{w}}^H(i)\bar{\mathbf{r}}(i)\}, \tag{6}$$

where $\mathbf{S}_D(i)$ denotes an $LP \times D$ projection matrix[2] which is applied to the received vector to extract the most important information from the data by performing dimensionality reduction, where $1 \le D < LP$, and $\bar{\mathbf{w}}(i) = [\bar{w}_0,\bar{w}_1,\ldots,\bar{w}_{D-1}]^T \in \mathbb{C}^{D\times 1}$ denotes the reduced-rank receive filter. In (6), for convenience, the $D \times 1$ projected received vector is denoted as

$$\bar{\mathbf{r}}(i) = \mathbf{S}_D^H(i)\mathbf{r}(i). \tag{7}$$

The basic problem in implementing the MSER reduced-rank receive processing scheme is how to effectively devise the projection matrix $\mathbf{S}_D(i)$ and the reduced-rank receive filter $\bar{\mathbf{w}}(i)$. In the following sections, we propose and investigate a new structure and adaptive algorithms for on-line estimation of these quantities based on the minimization of the SER cost function [7], [33]-[39].

## III. Proposed MSER-JPDF Reduced-Rank Linear Receive Processing Scheme

In this section, we detail the proposed MSER-JPDF reduced-rank linear receive processing scheme. Apart from the conventional reduced-rank techniques, the most direct method to reduce the dimensionality of the received vector is to decimate its content, i.e., to retain a subset of its elements while discarding the rest. However, this approach may entail a loss of information and therefore result in poor convergence performance. To overcome this problem, the proposed technique first performs a linear preprocessing operation on the received

[2]In this paper, projection simply refers to a linear transformation from a space of large dimension $LP$ to a space of smaller dimension $D$.

vector, then the output of the preprocessor is handled by a decimator, followed by a reduced-rank receive filter [23], [32]. With the aid of the linear preprocessing, essential information conveyed by the input signals can be preserved in the lower dimensional data vector operated upon by the reduced-rank receive filter. Since wireless channels tend to vary rapidly, and the determination of the optimal decimator is prohibitively complex due to the need for an exhaustive search, we propose to create several branches of preprocessing, decimation and reduced-rank receive filters based on a number of different fixed decimators [27]. For a given branch, the preprocessor and the reduced-rank receive filter are jointly designed according to the MSER criterion. The final symbol estimate is generated among the outputs of the multiple filtering branches according to the minimum Euclidean distance criterion.

### A. Overview of the MSER-JPDF Scheme

We design the subspace projection matrix $\mathbf{S}_D(i)$ by considering preprocessing and decimation. In this case, the receive filter length is substantially decreased (i.e., $D \ll L$), which in turn significantly reduces the computational complexity and leads to very fast training for large-scale multiple-antenna systems. The proposed MSER-JPDF scheme for the desired user is depicted in Fig. 1. The $LP \times 1$ received vector $\mathbf{r}(i)$ is processed by a parallel structure consisting of $B$ branches, where each branch contains a preprocessing filter and a decimation unit, followed by a reduced-rank receive filter. In the $l$-th branch, $l \in \{0, \ldots, B-1\}$, the received vector is operated by the preprocessor $\mathbf{p}_l(i) = [p_{0,l}(i), \ldots, p_{I-1,l}(i)]^T$ with length $I < LP$. The output of the preprocessor on the $l$-th branch is expressed as

$$\tilde{\mathbf{r}}_l(i) = \mathbf{P}_l^H(i)\mathbf{r}(i) \tag{8}$$

where the $LP \times LP$ Toeplitz convolution matrix $\mathbf{P}_l(i)$ is given by[3]

$$\mathbf{P}_l(i) = \begin{pmatrix} p_{0,l}(i) & 0 & \ldots & 0 \\ \vdots & p_{0,l}(i) & \ldots & 0 \\ p_{I-1,l}(i) & \vdots & \ldots & 0 \\ 0 & p_{I-1,l}(i) & \ldots & 0 \\ \vdots & \vdots & \ddots & \vdots \\ 0 & 0 & \ldots & p_{0,l}(i) \end{pmatrix}. \tag{9}$$

In order to facilitate the description of the scheme, we describe the vector $\tilde{\mathbf{r}}_l(i)$ as a function of the preprocessor vector $\mathbf{p}_l(i)$ and an input data matrix $\mathbf{R}(i)$ as follows:

$$\tilde{\mathbf{r}}_l(i) = \mathbf{P}_l^H(i)\mathbf{r}(i) = \mathbf{R}(i)\mathbf{p}_l^*(i) \tag{10}$$

where $(.)^*$ stands for the element-wise conjugate operation and the $LP \times I$ matrix $\mathbf{R}(i)$ is obtained from the received samples $\mathbf{r}(i) = [\mathbf{r}_0^T(i), \ldots, \mathbf{r}_{L-1}^T(i)]^T$ and has a Hankel structure shown in [27], [32] and [41].

The dimensionality reduction is performed by a decimation unit implemented as a $D \times LP$ decimation matrix $\mathbf{T}_l$ that projects $\tilde{\mathbf{r}}_l(i)$ onto the $D \times 1$ vector $\bar{\mathbf{r}}_l(i)$, where $D$ is the rank of $\mathbf{T}_l$. Specifically, the $D \times 1$ vector $\bar{\mathbf{r}}_l(i)$ for the $l$-th branch is given by

$$\bar{\mathbf{r}}_l(i) = \underbrace{\mathbf{T}_l\mathbf{P}_l^H(i)}_{\mathbf{S}_{D,l}^H(i)}\mathbf{r}(i) = \mathbf{T}_l\tilde{\mathbf{r}}_l(i) = \mathbf{T}_l\mathbf{R}(i)\mathbf{p}_l^*(i) \tag{11}$$

where $\mathbf{S}_{D,l}(i)$ denotes the equivalent subspace projection matrix. The output of the reduced-rank receive filter $\bar{\mathbf{w}}_l(i)$ corresponding to the $l$-th branch is given by

$$x_0^l(i) = \bar{\mathbf{w}}_l^H(i)\bar{\mathbf{r}}_l(i) \tag{12}$$

which is used in the minimization of the error probability for that branch.

As seen from Fig. 1, the proposed scheme employs $B$ parallel branches of preprocessors, decimators and receive filters. The optimum branch is selected according to the minimum Euclidean distance criterion, that is:

$$l_{opt} = \arg \min_{0 \le l \le B-1} |b_0(i) - x_0^l(i)|, \tag{13}$$

where $|.|$ represents the magnitude of a complex scalar and $b_0(i)$ refers to a known sequence of training symbols transmitted by the desired user and available at the receiver side. The output of the MSER-JPDF is given by

$$\hat{b}_0(i) = \mathcal{Q}\{x_0^{l_{opt}}(i)\} = \mathcal{Q}\{\bar{\mathbf{w}}_{l_{opt}}^H(i)\bar{\mathbf{r}}_{l_{opt}}(i)\}. \tag{14}$$

We can claim that more branches will result in better performance for the proposed algorithm. However, considering the affordable complexity, we have to configure the algorithm with the number of branches as small as possible and yet achieve a satisfactory performance. As will be shown in the simulation results, the proposed MSER-JPDF reduced-rank algorithm with the number of branches $B$ set to 4 offers an attractive tradeoff between performance and complexity.

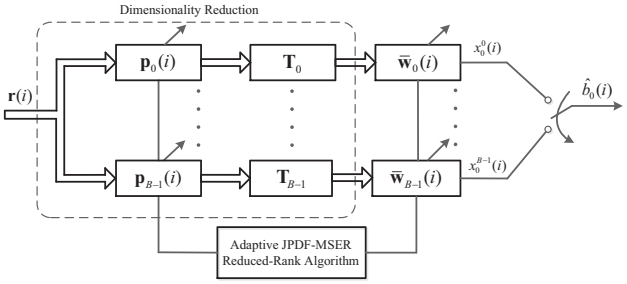


Fig. 1. Structure of the proposed MSER-JPDF scheme

### B. Design of the Decimation Unit

In this work, the elements of the decimation matrix only take the value 0 or 1, which corresponds to the decimation unit simply keeping or discarding its samples. The optimal decimation scheme exhaustively explores all possible patterns which select $D$ samples out of $LP$ samples. In this case, the design can be viewed as a combinatorial problem where the total number of patterns is $B = LP(LP-1)\ldots(LP-D+1)$. However, the optimal decimation scheme is too complex for practical use and several low-complexity approaches such

[3] Space-time processing is used in the current setting due to both inter-symbol and multiuser interferences. In this case, these interferences can be jointly suppressed by jointly processing the received signal in the temporal and spatial domains [24], [31].

as the uniform decimation, the pre-stored decimation and the random decimation have been investigated [28], [27]. Among these approaches, the pre-stored decimation provides a suboptimal solution to generate simple and yet effective decimation matrices. In this work, we therefore use the low-complexity pre-stored method, in which the $l$-th decimation matrix is formed as

$$\mathbf{T}_l = \left[ \begin{array}{cccc} \mathbf{t}_{l,0} & \mathbf{t}_{l,1} & \ldots & \mathbf{t}_{l,D-1} \end{array} \right]^T, \quad l \in \{0, \ldots, B-1\} \tag{15}$$

where the $LP \times 1$ vector $\mathbf{t}_{l,d}$ is composed of a single 1 and $LP-1$ 0s, as given by

$$\mathbf{t}_{l,d} = [\underbrace{0, \ldots, 0}_{v_{l,d}}, 1, \underbrace{0, \ldots, 0}_{LP-v_{l,d}-1}]^T, \quad d \in \{0, \ldots, D-1\} \tag{16}$$

and $v_{l,d}$ is the number of zeros before the non-zero entry. Hence, each row of decimation matrix $\mathbf{T}_l$ is all zero but for one entry which is set to 1; furthermore, we require that the ones in different row occupy different positions. Specifically, we set the values of $v_{l,d}$ in a deterministic way, which can be expressed as

$$v_{l,d} = \left\lfloor \frac{LP}{D} \right\rfloor d + l \tag{17}$$

where $\lfloor . \rfloor$ represents the floor function, which returns the largest integer that is smaller than or equal to its argument. The simulation results will show that the proposed MSER-JPDF reduced-rank scheme with the above suboptimal decimation scheme performs very well.

## IV. Proposed Adaptive Algorithms

In this section, we introduce the proposed adaptive MSER-JPDF reduced-rank algorithms. In particular, we develop the MSER-based adaptive algorithms to update the preprocessing filter $\mathbf{p}_l(i)$ and the reduced-rank receive filter $\bar{\mathbf{w}}_l(i)$ for each branch. Note that the subspace projection introduced in (11) is linear and hence, the transformed noise, i.e. $\mathbf{T}_l\mathbf{P}_l^H(i)\mathbf{n}(i)$, also follows a Gaussian distribution, allowing us to derive the MSER based algorithms. We first consider the case of BPSK symbols, and then extend the presentation to QAM symbols. The derivation is general in its conceptual approach and it could be extended to other modulation schemes. Subsequently, we propose an automatic parameter selection scheme to determine the lengths of the preprocessor and the reduced-rank receive filter during on-line operation.

### A. Adaptive MSER-JPDF Algorithm for BPSK Symbols

Firstly, let us consider the case with BPSK symbols. The symbol decision $\hat{b}_0(i)$ can be made as

$$\hat{b}_0(i) = \left\{ \begin{array}{ll} +1, & \text{if} \quad \Re[x_0^l(i)] \geq 0 \\ -1, & \text{if} \quad \Re[x_0^l(i)] < 0 \end{array} \right. \tag{18}$$

where $\Re[.]$ selects the real part and $x_0^l(i)$ is the output of the $l$-th branch as given in (12). Note that at the $i$-th block of transmitted symbols and for a given desired symbol $b_0(i)$, there are $N_b = 2^{(P+L_p-1)K-1}$ different possible arrangements (i.e. $((P+L_p-1)K-1)$-tuples) of the binary multiuser interference (MUI) symbols $b_k(i-\mu)$, where $k \in \{1, \ldots, K-1\}$ and $\mu \in \{0, \ldots, P+L_p-2\}$, and the binary intersymbol interference (ISI) symbols $b_0(i-\mu^{'})$, where $\mu^{'} \in \{1, \ldots, P+L_p-2\}$. Then, we define a set:

$$\mathcal{X} = \{\tilde{\mathbf{b}}^0, \tilde{\mathbf{b}}^1, \ldots, \tilde{\mathbf{b}}^{N_b-1}\} \tag{19}$$

which contains all possible transmitted symbol vectors of size $K(P+L_p-1)\times 1$ for a given $b_0(i)$. The noise-free component of the reduced-rank receive filter corresponding to the $l$-th branch takes its value from the set

$$\mathcal{Y} = \{\bar{x}_0^{l,q} = \bar{\mathbf{w}}_l^H(i)\mathbf{T}_l\mathbf{P}_l^H(i)\mathbf{H}(i)\tilde{\mathbf{b}}^q : \ 0 \leq q \leq N_b-1\} \tag{20}$$

where $\tilde{\mathbf{b}}^q \in \mathcal{X}$. Based on the Gaussian distribution for the additive noise in (2) and assuming an equiprobable model for the $N_b$ possible transmit vectors $\tilde{\mathbf{b}}^q$, we can express the probability density function (PDF) for the real part of the reduced-rank receive filter output corresponding to the $l$-th branch, conditioned on the desired symbol $b_0(i)$, as

$$\begin{aligned} f_l(x|b_0(i)) = & \frac{1}{N_b\sigma\sqrt{2\pi\bar{\mathbf{w}}_l^H(i)\mathbf{T}_l\mathbf{P}_l^H(i)\mathbf{P}_l(i)\mathbf{T}_l^H\bar{\mathbf{w}}_l(i)}} \\ & \times \sum_{q=0}^{N_b-1} e^{-\frac{|x-\Re[\bar{x}_0^{l,q}]|^2}{2\sigma^2\bar{\mathbf{w}}_l^H(i)\mathbf{T}_l\mathbf{P}_l^H(i)\mathbf{P}_l(i)\mathbf{T}_l^H\bar{\mathbf{w}}_l(i)}} \end{aligned} \tag{21}$$

where $\bar{x}_0^{l,q} \in \mathcal{Y}$. In practice, the PDF of the reduced-rank receive filter output should be estimated using kernel density estimation [88] based on a block of experimental data. Specifically, given $J$ observations of the array output vector, denoted as $\mathbf{r}^\nu$ where $\nu \in \{0, 1, \ldots, J-1\}$, a kernel estimate of the true PDF is given by

$$\begin{aligned} \tilde{f}_l(x|b_0(i)) = & \frac{1}{J\rho\sqrt{2\pi\bar{\mathbf{w}}_l^H(i)\mathbf{T}_l\mathbf{P}_l^H(i)\mathbf{P}_l(i)\mathbf{T}_l^H\bar{\mathbf{w}}_l(i)}} \\ & \times \sum_{\nu=0}^{J-1} e^{-\frac{|x-\Re[x_0^{l,\nu}]|^2}{2\rho^2\bar{\mathbf{w}}_l^H(i)\mathbf{T}_l\mathbf{P}_l^H(i)\mathbf{P}_l(i)\mathbf{T}_l^H\bar{\mathbf{w}}_l(i)}} \end{aligned} \tag{22}$$

where $\rho$ represents the radius parameter or width of the kernel density estimate and $x_0^{l,\nu}$ denotes the output of the $l$-th branch reduced-rank receive filter corresponding to the $\nu$-th testing vector $\mathbf{r}^\nu$. In order to design a practical on-line adaptive algorithm with moderate complexity, we consider the following single-sample estimate of the true PDF[4]

$$\tilde{f}_l(x|b_0(i)) = \frac{1}{\sqrt{2\pi}\rho} e^{-\frac{|x-\Re[x_0^l(i)]|^2}{2\rho^2}}. \tag{23}$$

Subsequently, based on the PDF estimate (23) we obtain the instantaneous SER estimate corresponding to the $l$-th branch of the proposed reduced-rank scheme, as given by (24). In order to simplify this expression, we define a new quantity $s = \frac{x-\Re[x_0^l(i)]}{\sqrt{2}\rho}$. Then, we can express the BPSK SER by means of the following unified expression:

$$\mathcal{P}_e^l(\bar{\mathbf{w}}_l(i), \mathbf{p}_l(i)) = \int_{-\infty}^{\frac{-\Re[x_0^l(i)]\text{sign}(b_0(i))}{\sqrt{2}\rho}} \frac{1}{\sqrt{\pi}} e^{-s^2} ds \tag{25}$$

[4]As discussed in [7], [34], [35], the SER does not change significantly with the quantity $\bar{\mathbf{w}}_l^H(i)\mathbf{T}_l\mathbf{P}_l^H(i)\mathbf{P}_l(i)\mathbf{T}_l^H\bar{\mathbf{w}}_l(i)$. Therefore, in order to simplify the gradient of the resulting estimated SER, we can drop the term $\bar{\mathbf{w}}_l^H(i)\mathbf{T}_l\mathbf{P}_l^H(i)\mathbf{P}_l(i)\mathbf{T}_l^H\bar{\mathbf{w}}_l(i)$ and employ a constant kernel width $\rho$, which leads to significant reductions in computational complexity.

$$\mathcal{P}_e^l(\bar{\mathbf{w}}_l(i),\mathbf{p}_l(i)) = \begin{cases} \int_{-\infty}^{0} \frac{1}{\sqrt{2\pi}\rho} e^{-\frac{|x-\Re[x_0^l(i)]|^2}{2\rho^2}} dx, & \text{if} \quad b_0(i) = +1 \\ \int_{0}^{\infty} \frac{1}{\sqrt{2\pi}\rho} e^{-\frac{|x-\Re[x_0^l(i)]|^2}{2\rho^2}} dx, & \text{if} \quad b_0(i) = -1 \end{cases} \tag{24}$$

TABLE I
ADAPTIVE MSER-JPDF REDUCED-RANK ALGORITHM FOR BPSK SYMBOLS

| | |
|---|---|
| 1 | Set step-size values $\mu_w$ and $\mu_{S_D}$ and the number of branches $B$. |
| 2 | Initialize $\bar{\mathbf{w}}_l(0)$ and $\mathbf{p}_l(0)$. Set $\mathbf{T}_0, \ldots, \mathbf{T}_{B-1}$. |
| 3 | for time instant $i \in \{0, 1, \ldots\}$ do |
| 4 | for $l \in \{0, \ldots, B-1\}$ do |
| 5 | Compute $\mathbf{p}_l(i+1)$ based on (31) using $\bar{\mathbf{w}}_l(i)$ and $\mathbf{T}_l$. |
| 6 | Compute $\bar{\mathbf{w}}_l(i+1)$ based on (30) using $\mathbf{p}_l(i+1)$ and $\mathbf{T}_l$. |
| 7 | end |
| 8 | Select the optimal branch $l_{opt} = \arg\min_{0 \le l \le B-1} \lvert b_0(i) - x_0^l(i) \rvert$, where $x_0^l(i) = \bar{\mathbf{w}}_l^H(i+1)\mathbf{T}_l\mathbf{P}_l^H(i+1)\mathbf{r}(i)$. |
| | Generate the estimate symbol corresponding to branch $l_{opt}$: $\hat{b}_0(i) = \mathcal{Q}\{x_0^{l_{opt}}(i)\}$. |

where sign(.) denotes the signum function.

In the following, we derive the gradient terms for the reduced-rank receive filter and the preprocessing vector for each branch. By computing the gradient of (25) with respect to $\bar{\mathbf{w}}_l^*(i)$ and after further mathematical manipulations we obtain

$$\frac{\partial \mathcal{P}_e^l(\bar{\mathbf{w}}_l(i),\mathbf{p}_l(i))}{\partial \bar{\mathbf{w}}_l^*} = -\text{sign}(b_0(i)) \frac{1}{\sqrt{2\pi}\rho} e^{-\frac{|\Re[x_0^l(i)]|^2}{2\rho^2}} \times \mathbf{T}_l\mathbf{P}_l^H(i)\mathbf{r}(i). \tag{26}$$

In order to derive the gradient terms for the preprocessor $\mathbf{p}_l(i)$, we define the $LP \times 1$ vector $\mathbf{T}_l^H\bar{\mathbf{w}}_l(i) = [d_0(i), d_1(i), \ldots, d_{LP-1}(i)]^T$. The reduced-rank receive filter output can be rewritten as

$$x_0^l(i) = \bar{\mathbf{w}}_l^H(i)\mathbf{T}_l\mathbf{P}_l^H(i)\mathbf{r}(i) = \mathbf{p}_l^H(i)\mathbf{D}^H(i)\mathbf{r}(i), \tag{27}$$

where the $LP \times I$ matrix $\mathbf{D}(i)$ has the following structure

$$\mathbf{D}(i) = \begin{pmatrix} d_0(i) & 0 & \ldots & 0 \\ d_1(i) & d_0(i) & \ldots & 0 \\ \vdots & \vdots & \ddots & \vdots \\ d_{I-1}(i) & d_{I-2}(i) & \ldots & d_0(i) \\ d_I(i) & d_{I-1}(i) & \ldots & d_1(i) \\ \vdots & \vdots & \ddots & \vdots \\ d_{LP-1}(i) & d_{LP-2}(i) & \ldots & d_{LP-I}(i) \end{pmatrix}. \tag{28}$$

By computing the gradient of (25) with respect to $\mathbf{p}_l^*(i)$, we obtain

$$\frac{\partial \mathcal{P}_e^l(\bar{\mathbf{w}}_l(i),\mathbf{p}_l(i))}{\partial \mathbf{p}_l^*} = -\text{sign}(b_0(i)) \frac{1}{\sqrt{2\pi}\rho} e^{-\frac{|\Re[x_0^l(i)]|^2}{2\rho^2}} \times \mathbf{D}^H(i)\mathbf{r}(i). \tag{29}$$

The preprocessing filter and the reduced-rank receive filter are jointly optimized according to the MSER criterion [7], [35]. The proposed SG update equations for the $l$-th branch for BPSK symbols are obtained by substituting the gradient terms (26) and (29) in the following expressions

$$\bar{\mathbf{w}}_l(i+1) = \bar{\mathbf{w}}_l(i) - \mu_w \frac{\partial \mathcal{P}_e^l(\bar{\mathbf{w}}_l(i),\mathbf{p}_l(i))}{\partial \bar{\mathbf{w}}_l^*} \tag{30}$$

and

$$\mathbf{p}_l(i+1) = \mathbf{p}_l(i) - \mu_p \frac{\partial \mathcal{P}_e^l(\bar{\mathbf{w}}_l(i),\mathbf{p}_l(i))}{\partial \mathbf{p}_l^*}, \tag{31}$$

where $\mu_w$ and $\mu_p$ are the step-size values. At each time instant, these two vectors for a given branch $l$ are updated in an alternating way. The algorithm is devised to start its operation in the training (TR) mode, where a known training sequence $b_0(i)$ is employed, and then to switch to the decision-directed (DD) mode, where the estimated symbols $\hat{b}_0(i)$ from (18) are used to compute the gradients in (26) and (29). Expressions (30) and (31) need initial values, that is $\bar{\mathbf{w}}_l(0)$ and $\mathbf{p}_l(0)$. The proposed MSER-JPDF algorithm for BPSK modulation is summarized in Table I.

### *B. Adaptive MSER-JPDF Algorithm for QAM Symbols*

Let us consider the case with $M$-ary QAM symbols. For the proposed reduced-rank scheme, the symbol error probability regarding the $l$-th branch can be represented as

$$\mathcal{P}_e^l(\bar{\mathbf{w}}_l(i),\mathbf{p}_l(i)) = \mathcal{P}_e^{l,R}(\bar{\mathbf{w}}_l(i),\mathbf{p}_l(i)) + \mathcal{P}_e^{l,I}(\bar{\mathbf{w}}_l(i),\mathbf{p}_l(i)) - \mathcal{P}_e^{l,R}(\bar{\mathbf{w}}_l(i),\mathbf{p}_l(i))\mathcal{P}_e^{l,I}(\bar{\mathbf{w}}_l(i),\mathbf{p}_l(i)) \tag{32}$$

where $\mathcal{P}_e^l(\bar{\mathbf{w}}_l(i),\mathbf{p}_l(i)) = \text{Prob}\{b_0(i) \neq \hat{b}_0(i)\}$ denotes the total SER while $\mathcal{P}_e^{l,R}(\bar{\mathbf{w}}_l(i),\mathbf{p}_l(i)) = \text{Prob}\{\Re[b_0(i)] \neq \Re[\hat{b}_0(i)]\}$ and $\mathcal{P}_e^{l,I}(\bar{\mathbf{w}}_l(i),\mathbf{p}_l(i)) = \text{Prob}\{\Im[b_0(i)] \neq \Im[\hat{b}_0(i)]\}$ denote the real part and imaginary part SERs, respectively (here, $\Im[.]$ selects the imaginary part). The optimization problem is formulated to minimize an upper bound of the SER as follows [7]:

$$\min_{\bar{\mathbf{w}}_l(i),\mathbf{p}_l(i)} \bar{\mathcal{P}}_e^l(\bar{\mathbf{w}}_l(i),\mathbf{p}_l(i)) \tag{33}$$

where $\bar{\mathcal{P}}_e^l(\bar{\mathbf{w}}_l(i),\mathbf{p}_l(i)) = \mathcal{P}_e^{l,R}(\bar{\mathbf{w}}_l(i),\mathbf{p}_l(i)) + \mathcal{P}_e^{l,I}(\bar{\mathbf{w}}_l(i),\mathbf{p}_l(i))$. For small values of SER, since the true SER $\mathcal{P}_e^l(\bar{\mathbf{w}}_l(i),\mathbf{p}_l(i))$ is quite close to the upper bound $\bar{\mathcal{P}}_e^l(\bar{\mathbf{w}}_l(i),\mathbf{p}_l(i))$, the solution obtained by minimizing (33) is practically relevant and thus we pursue this strategy.

The output of the reduced-rank receive filter corresponding

$$\hat{b}_0^R(i) = \begin{cases} F_1, & \text{if } \Re[x_0^l(i)] \le \omega_{0,0}^l(i)(F_1+1) \\ F_m, & \text{if } \omega_{0,0}^l(i)(F_m-1) < \Re[x_0^l(i)] \le \omega_{0,0}^l(i)(F_m+1),\ 2 \le m \le \sqrt{M}-1 \\ F_{\sqrt{M}}, & \text{if } \Re[x_0^l(i)] > \omega_{0,0}^l(i)(F_{\sqrt{M}}-1) \end{cases} \tag{37}$$

$$\hat{b}_0^I(i) = \begin{cases} F_1, & \text{if } \Im[x_0^l(i)] \le \omega_{0,0}^l(i)(F_1+1) \\ F_n, & \text{if } \omega_{0,0}^l(i)(F_n-1) < \Im[x_0^l(i)] \le \omega_{0,0}^l(i)(F_n+1),\ 2 \le n \le \sqrt{M}-1 \\ F_{\sqrt{M}}, & \text{if } \Im[x_0^l(i)] > \omega_{0,0}^l(i)(F_{\sqrt{M}}-1) \end{cases} \tag{38}$$

to the $l$-th branch can be expressed as

$$\begin{aligned} x_0^l(i) = \omega_{0,0}^l(i)b_0(i) + \overbrace{\sum_{\mu=1}^{P+L_p-2} \omega_{0,\mu}^l(i)b_0(i-\mu)}^{\textit{residual ISI}} \\ + \overbrace{\sum_{k=1}^{K-1}\sum_{\mu=0}^{P+L_p-2} \omega_{k,\mu}^l(i)b_k(i-\mu)}^{\textit{residual MUI}} + e(i). \end{aligned} \tag{34}$$

In this expression, we have $\omega_{k,\mu}^l(i) = \bar{\mathbf{w}}_l^H(i)\mathbf{T}_l\mathbf{P}_l^H(i)\mathbf{h}_{k,\mu}(i)$, where $\mathbf{h}_{k,\mu}(i)$ denotes the $\mu$-th column vector of matrix $[\mathbf{H}_{0,k}^T(i),\ldots,\mathbf{H}_{L-1,k}^T(i)]^T$, $\mu \in \{0,\ldots,P+L_p-2\}$, $k \in \{0,\ldots,K-1\}$, while the term $e(i) = \bar{\mathbf{w}}_l^H(i)\mathbf{T}_l\mathbf{P}_l^H(i)\mathbf{n}(i)$. Note that the multiplier of the desired symbol, i.e., $\omega_{0,0}^l(i)$ in (34) is a complex number which can be represented as $\omega_{0,0}^l(i) = \bar{\mathbf{w}}_l^H(i)\mathbf{T}_l\mathbf{P}_l^H(i)\mathbf{h}_{0,0}(i) = \mathbf{p}_l^H(i)\mathbf{D}^H(i)\mathbf{h}_{0,0}(i)$. To simplify the detection of $M$-QAM symbols, we apply the following phase rotation operations to transform these complex multipliers into real and positive quantities, which in effect corresponds to the substitution

$$\bar{\mathbf{w}}_l(i) \leftarrow \frac{\omega_{0,0}^l(i)}{|\omega_{0,0}^l(i)|}\bar{\mathbf{w}}_l(i) \tag{35}$$

or

$$\mathbf{p}_l(i) \leftarrow \frac{\omega_{0,0}^l(i)}{|\omega_{0,0}^l(i)|}\mathbf{p}_l(i). \tag{36}$$

By using (35) for the reduced-rank receive filter or (36) for the preprocessing filter, we have equivalently $\omega_{0,0}^{l,R}(i) > 0$ and $\omega_{0,0}^{l,I}(i) = 0$, where $\omega_{0,0}^{l,R}(i)$ and $\omega_{0,0}^{l,I}(i)$ represent the real and imaginary parts of $\omega_{0,0}^l(i)$ after phase rotation, respectively. Hence, the symbol decision $\hat{b}_0(i) = \hat{b}_0^R(i) + j\hat{b}_0^I(i)$ can be made as (37) and (38), where $\hat{b}_0^R(i)$ and $\hat{b}_0^I(i)$ represent the real and imaginary parts of the estimated $M$-QAM symbol, respectively.

We focus on the real part SER, i.e. $\mathcal{P}_e^{l,R}(\bar{\mathbf{w}}_l(i),\mathbf{p}_l(i))$, to introduce the proposed algorithm; the derivation regarding the imaginary part SER is straightforward. In this case, we have $N_d = M^{(P+L_p-1)K-1}$ different possible arrangements in total for the MUI and ISI symbols. Similar to the BPSK case, for a given $b_0(i)$ we define two sets as follows:

$$\bar{\mathcal{X}} = \{\tilde{\mathbf{b}}^0, \tilde{\mathbf{b}}^1, \ldots, \tilde{\mathbf{b}}^{N_d-1}\} \tag{39}$$

$$\bar{\mathcal{Y}} = \{\bar{x}_0^{l,q} = \bar{\mathbf{w}}_l^H(i)\mathbf{T}_l\mathbf{P}_l^H(i)\tilde{\mathbf{H}}(i)\tilde{\mathbf{b}}^q :\ 0 \le q \le N_d-1\}. \tag{40}$$

The conditional PDF of the real part of the reduced-rank receive filter output for branch $l$ is given by

$$\begin{aligned} f_l(x|b_0(i)) = \frac{1}{N_d\sigma\sqrt{2\pi\bar{\mathbf{w}}_l^H(i)\mathbf{T}_l\mathbf{P}_l^H(i)\mathbf{P}_l(i)\mathbf{T}_l^H\bar{\mathbf{w}}_l(i)}} \\ \times \sum_{q=0}^{N_d-1} e^{-\frac{|x-\Re[\bar{x}_0^{l,q}]|^2}{2\sigma^2\bar{\mathbf{w}}_l^H(i)\mathbf{T}_l\mathbf{P}_l^H(i)\mathbf{P}_l(i)\mathbf{T}_l^H\bar{\mathbf{w}}_l(i)}} \end{aligned} \tag{41}$$

where $\bar{x}_0^{l,q} \in \bar{\mathcal{Y}}$. By using the kernel density estimation, the single-sample estimate of the PDF similar to (23) can be obtained. Based on the discussion in [7], the SER expression of the real part for branch $l$ is given by

$$\mathcal{P}_e^{l,R}(\bar{\mathbf{w}}_l(i),\mathbf{p}_l(i)) = \phi\int_{-\infty}^{\omega_{0,0}^l(i)(\Re[b_0(i)]-1)} \frac{1}{\sqrt{2\pi}\rho}e^{-\frac{|x-\Re[x_0^l(i)]|^2}{2\rho^2}}dx \tag{42}$$

where $\phi = \frac{2\sqrt{M}-2}{\sqrt{M}}$. Then, introducing $s = \frac{x-\Re[x_0^l(i)]}{\sqrt{2}\rho}$, (42) can be rewritten as

$$\mathcal{P}_e^{l,R}(\bar{\mathbf{w}}_l(i),\mathbf{p}_l(i)) = \phi\int_{-\infty}^{\frac{\omega_{0,0}^l(i)(\Re[b_0(i)]-1)-\Re[x_0^l(i)]}{\sqrt{2}\rho}} \frac{1}{\sqrt{\pi}}e^{-|s|^2}ds. \tag{43}$$

Note that $\omega_{0,0}^l(i)$ and $x_0^l(i)$ are both functions of $\bar{\mathbf{w}}_l(i)$ and $\mathbf{p}_l(i)$. By taking the gradient of (43) with respect to $\bar{\mathbf{w}}_l^*(i)$ and $\mathbf{p}_l^*(i)$, respectively, we obtain

$$\begin{aligned} \frac{\partial\mathcal{P}_e^{l,R}(\bar{\mathbf{w}}_l(i),\mathbf{p}_l(i))}{\partial\bar{\mathbf{w}}_l^*} = \frac{\phi}{\sqrt{2\pi}\rho}e^{-\frac{|\omega_{0,0}^l(i)(\Re[b_0(i)]-1)-\Re[x_0^l(i)]|^2}{2\rho^2}} \\ \times \mathbf{T}_l\mathbf{P}_l^H(i)\big((\Re[b_0(i)]-1)\mathbf{h}_{0,0}(i) - \mathbf{r}(i)\big) \end{aligned} \tag{44}$$

and

$$\begin{aligned} \frac{\partial\mathcal{P}_e^{l,R}(\bar{\mathbf{w}}_l(i),\mathbf{p}_l(i))}{\partial\mathbf{p}_l^*} = \frac{\phi}{\sqrt{2\pi}\rho}e^{-\frac{|\omega_{0,0}^l(i)(\Re[b_0(i)]-1)-\Re[x_0^l(i)]|^2}{2\rho^2}} \\ \times \mathbf{D}^H(i)\big((\Re[b_0(i)]-1)\mathbf{h}_{0,0}(i) - \mathbf{r}(i)\big). \end{aligned} \tag{45}$$

Following a similar approach, we can obtain the SER expression of the imaginary part corresponding to the $l$-th branch as

$$\mathcal{P}_e^{l,I}(\bar{\mathbf{w}}_l(i),\mathbf{p}_l(i)) = \phi\int_{-\infty}^{\omega_{0,0}^l(i)(\Im[b_0(i)]-1)} \frac{1}{\sqrt{2\pi}\rho}e^{-\frac{|x-\Im[x_0^l(i)]|^2}{2\rho^2}}dx. \tag{46}$$

The gradient terms of this expression with respect $\bar{\mathbf{w}}_l(i)$ and $\mathbf{p}_l(i)$ are given by

$$\begin{aligned} \frac{\partial\mathcal{P}_e^{l,I}(\bar{\mathbf{w}}_l(i),\mathbf{p}_l(i))}{\partial\bar{\mathbf{w}}_l^*} = \frac{\phi}{\sqrt{2\pi}\rho}e^{-\frac{|\omega_{0,0}^l(i)(\Im[b_0(i)]-1)-\Im[x_0^l(i)]|^2}{2\rho^2}} \\ \times \mathbf{T}_l\mathbf{P}_l^H(i)\big(j\mathbf{r}(i) + (\Im[b_0(i)]-1)\mathbf{h}_{0,0}(i)\big) \end{aligned} \tag{47}$$

$$\bar{\mathbf{w}}_l^{D_{max}}(i) = [\bar{w}_{l,0}(i), \bar{w}_{l,1}(i), \ldots, \bar{w}_{l,D_{min}-1}(i), \ldots, \bar{w}_{l,D_{max}-1}(i)]^T \tag{51}$$

$$\mathbf{p}_l^{I_{max}}(i) = [p_{l,0}(i), p_{l,1}(i), \ldots, p_{l,I_{min}-1}(i), \ldots, p_{l,I_{max}-1}(i)]^T. \tag{52}$$

TABLE II
ADAPTIVE MSER-JPDF REDUCED-RANK ALGORITHM FOR QAM SYMBOLS

| | |
|---|---|
| 1 | Set step-size values $\mu_w$ and $\mu_{S_D}$ and the number of branches $B$. |
| 2 | Initialize $\bar{\mathbf{w}}_l(0)$, $\mathbf{p}_l(0)$ and $\omega_{0,0}^l(0)$. Set $\mathbf{T}_0, \ldots, \mathbf{T}_{B-1}$. |
| 3 | for time instant $i \in \{0, 1, \ldots\}$ do |
| 4 | for $l \in \{0, \ldots, B-1\}$ do |
| 5 | Compute $\mathbf{p}_l(i+1)$ based on (50) using $\omega_{0,0}^l(i)$, $\mathbf{T}_l$ and $\bar{\mathbf{w}}_l(i)$. |
| 6 | Compute $\omega_{0,0}^l(i)$ based on $\omega_{0,0}^l(i) = \mathbf{p}_l^H(i+1)\mathbf{D}^H(i)\mathbf{h}_{0,0}(i)$. |
| | Adjust $\mathbf{p}_l(i+1)$ by using $\mathbf{p}_l(i+1) \leftarrow \frac{\omega_{0,0}^l(i)}{\lvert\omega_{0,0}^l(i)\rvert}\mathbf{p}_l(i+1)$. |
| 7 | Compute $\bar{\mathbf{w}}_l(i+1)$ based on (49) using $\omega_{0,0}^l(i)$, $\mathbf{T}_l$ and $\mathbf{p}_l(i+1)$. |
| 8 | Compute $\omega_{0,0}^l(i+1)$ based on $\omega_{0,0}^l(i+1) = \bar{\mathbf{w}}_l^H(i+1)\mathbf{T}_l\mathbf{P}_l^H(i+1)\mathbf{h}_{0,0}(i)$. |
| | Adjust $\bar{\mathbf{w}}_l(i+1)$ by using $\bar{\mathbf{w}}_l(i+1) \leftarrow \frac{\omega_{0,0}^l(i+1)}{\lvert\omega_{0,0}^l(i+1)\rvert}\bar{\mathbf{w}}_l(i+1)$. |
| 9 | end |
| 10 | Select the optimal branch $l_{opt} = \arg\min_{0\le l\le B-1} \lvert b_0(i) - x_0^l(i)\rvert$, where $x_0^l(i) = \bar{\mathbf{w}}_l^H(i+1)\mathbf{T}_l\mathbf{P}_l^H(i+1)\mathbf{r}(i)$. |
| | Generate the estimate symbol corresponding to branch $l_{opt}$: $\hat{b}_0(i) = \mathcal{Q}\{x_0^{l_{opt}}(i)\}$. |

and

$$\frac{\partial \mathcal{P}_e^{l,I}(\bar{\mathbf{w}}_l(i), \mathbf{p}_l(i))}{\partial \mathbf{p}_l^*} = \frac{\phi}{\sqrt{2\pi}\rho} e^{-\frac{|\omega_{0,0}^l(i)(\Im[b_0(i)]-1) - \Im[x_0^l(i)]|^2}{2\rho^2}} \times \mathbf{D}^H(i)\big(j\mathbf{r}(i) + (\Im[b_0(i)] - 1)\mathbf{h}_{0,0}(i)\big). \tag{48}$$

Next, the preprocessing filter and the reduced-rank receive filter are jointly optimized using recursions that are employed in an alternating fashion. The proposed SG update equations corresponding to branch $l$ for QAM symbols can be obtained by substituting the gradient terms (44), (45), (47) and (48) in the following expressions:

$$\bar{\mathbf{w}}_l(i+1) = \bar{\mathbf{w}}_l(i) - \mu_w\left(\frac{\partial \mathcal{P}_e^{l,R}(\bar{\mathbf{w}}_l(i), \mathbf{p}_l(i))}{\partial \bar{\mathbf{w}}_l^*} + \frac{\partial \mathcal{P}_e^{l,I}(\bar{\mathbf{w}}_l(i), \mathbf{p}_l(i))}{\partial \bar{\mathbf{w}}_l^*}\right) \tag{49}$$

and

$$\mathbf{p}_l(i+1) = \mathbf{p}_l(i) - \mu_p\left(\frac{\partial \mathcal{P}_e^{l,R}(\bar{\mathbf{w}}_l(i), \mathbf{p}_l(i))}{\partial \mathbf{p}_l^*} + \frac{\partial \mathcal{P}_e^{l,I}(\bar{\mathbf{w}}_l(i), \mathbf{p}_l(i))}{\partial \mathbf{p}_l^*}\right). \tag{50}$$

Similar to the proposed adaptive algorithm for BPSK symbols, in this case the algorithm is developed to start in the TR mode, and then to switch to the DD mode. The proposed MSER-JPDF algorithm for $M$-QAM symbols is summarized in Table II[5], where the arrow denotes an overwrite operation.

[5]Note that the proposed adaptive algorithms can be extended to multicarrier systems (e.g. filter-bank multicarrier and generalized orthogonal frequency-division multiplexing (OFDM) systems that are being considered for 5G). With multicarrier modulation, the system can be described with a flat fading channel for each subcarrier and the proposed scheme and algorithms would mitigate the MUI rather than both ISI and MUI, as with the current description.

### C. Automatic Parameter Selection

Since the performance of the adaptive MSER-JPDF reduced-rank algorithm depends on the rank $D$ and the length of the preprocessor $I$, we develop an automatic parameter selection scheme in which $D$ and $I$ are adjusted on-line for added flexibility in the implementation of the proposed structure. The proposed scheme performs the search within a range of appropriate values and relies on the Euclidean distance to determine the lengths of $\bar{\mathbf{w}}_l(i)$ and $\mathbf{p}_l(i)$ corresponding to branch $l$, which can be adjusted in a flexible structure. At each time instant, for branch $l$ we adapt a reduced-rank receive filter $\bar{\mathbf{w}}_l^{D_{max}}(i)$ and a preprocessor $\mathbf{p}_l^{I_{max}}(i)$ according to the proposed algorithms in Table I or II with the maximum allowed rank $D_{max}$ and the maximum preprocessor length $I_{max}$, respectively, which can be expressed as (51) and (52). Then, we test the values of rank $D$ and preprocessor length $I$ within the range, namely, $D_{min} \le D \le D_{max}$ and $I_{min} \le I \le I_{max}$. For each pair of $D$ and $I$ of branch $l$, we substitute the vectors $\bar{\mathbf{w}}_l^{(D)}(i) = [\bar{w}_{l,0}(i), \ldots, \bar{w}_{l,D-1}(i)]^T$ and $\mathbf{p}_l^{(I)}(i) = [p_{l,0}(i), \ldots, p_{l,I-1}(i)]^T$, whose components are taken from $\bar{\mathbf{w}}_l^{D_{max}}(i)$ and $\mathbf{p}_l^{I_{max}}(i)$ in (51) and (52), into the following expression of the Euclidean distance

$$\varepsilon_l^{D,I}(i) = |b_0(i) - \bar{\mathbf{w}}_l^{(D)H}(i)\mathbf{T}_l\mathbf{R}(i)\mathbf{p}_l^{(I)*}(i)|. \tag{53}$$

The optimum lengths $D_{l,opt}$ and $I_{l,opt}$ for the reduced-rank receive filter and the preprocessor corresponding to branch $l$ at time instant $i$ can be chosen as follows:

$$[D_{l,opt}, I_{l,opt}] = \arg \min_{\substack{D_{min}\le D\le D_{max} \\ I_{min}\le I\le I_{max}}} \varepsilon_l^{D,I}(i). \tag{54}$$

After the optimum filter lengths are determined for all the branches, we select the optimum branch of the JPDF scheme based on the following criterion

$$l_{opt} = \arg \min_{0\le l\le B-1} |b_0(i) - \bar{\mathbf{w}}_l^{(D_{l,opt})H}(i)\mathbf{T}_l\mathbf{R}(i)\mathbf{p}_l^{(I_{l,opt})*}(i)|. \tag{55}$$

TABLE III
COMPUTATIONAL COMPLEXITY IN THE CASE OF BPSK

| Algorithm | Number of operations per symbol | |
|---|---|---|
| | Multiplications | Additions |
| Full-Rank-LMS | $2LP+1$ | $2LP$ |
| Full-Rank-MSER [35] | $3LP+1$ | $2LP$ |
| MSER-JIO [40] | $8LPD+7D+2LP+9$ | $7LPD+2LP-1$ |
| EIG [13] | $O((LP)^3)$ | $O((LP)^3)$ |
| MSER-MSWF [38] | $D(LP)^2+4LPD+5D+LP+7$ | $D(LP)^2+5LPD-1$ |
| MSER-JPDF | $BI(LP+1.5)+BD(I+2)+6B-0.5I^2B$ | $BI(LP+0.5)+BD(I+1)-0.5I^2B$ |

TABLE IV
COMPUTATIONAL COMPLEXITY IN THE CASE OF QAM

| Algorithm | Number of operations per symbol | |
|---|---|---|
| | Multiplications | Additions |
| Full-Rank-LMS | $2LP+1$ | $2LP$ |
| Full-Rank-MSER [7] | $6LP+5$ | $5LP$ |
| MSER-JIO [40] | $10LPD+7D+4LP+17$ | $9LPD+4LP+3$ |
| EIG [13] | $O((LP)^3)$ | $O((LP)^3)$ |
| MSER-MSWF [38] | $D(LP)^2+5LPD+5D+2LP+11$ | $D(LP)^2+6LPD+LP+1$ |
| MSER-JPDF | $BI(2LP+3)+2BD(2I+1)+8B-BI^2$ | $2BI(LP+1)+BD(4I-1)+2BLP-BI^2$ |

Hence, in this case the output of the proposed reduced-rank scheme at time instant $i$ is generated according to the selected branch $l_{opt}$ with the optimum parameters. For given lengths $D_{max}$ and $I_{max}$, the complexity of the automatic parameter selection scheme mainly lies in the computation of the distance $\varepsilon_l^{D,I}(i)$ in (53) and a simple search over the candidates $D$ and $I$ in (54). Consequently, this approach does not considerably increase the computational complexity. Note that the smaller values of $D$ and $I$ may produce faster adaptation during the initial stage of the estimation procedure while slightly larger values of $D$ and $I$ usually yield better steady-state performance. In Section VI, we will show that the proposed adaptive MSER-JPDF reduced-rank algorithms with the automatic parameter scheme can improve the convergence speed and steady-state performance compared to the algorithms with fixed parameters $D$ and $I$.

## V. ANALYSIS OF THE PROPOSED ALGORITHMS

In this section, we carry out the analysis of the proposed MSER-JPDF adaptive reduced-rank algorithms. Firstly, we compare the computational complexity of these new algorithms to that of existing reduced-rank adaptive algorithms and of the conventional full-rank adaptive algorithms. Secondly, we investigate the convergence behavior of the newly proposed algorithms.

### A. Computational Complexity

In Table III, we focus on the case of BPSK and show the number of additions and multiplications per symbol of the proposed adaptive reduced-rank algorithm, the existing adaptive MSER-based reduced-rank algorithms [38], [40], the conventional adaptive LMS full-rank algorithm [11] and the adaptive full-rank algorithm based on the SER criterion [35]. Table IV shows the corresponding figures for the case of QAM symbols. The overall complexity of the proposed algorithm includes the complexity of the selection mechanism and the design complexity of each branch multiplied by the number of branches $B$. In practice, to limit computational complexity, the number of branches should be kept small, typically $B \in \{2,3,4\}$ in this work. From the figures in these Tables, it is clear that the full-rank SG-based algorithms have lower complexity than all the reduced-rank algorithms under comparison. As pointed out earlier, the main problem of the full-rank SG-based adaptive filtering algorithms is their very slow convergence performance when a filter with a large number of adaptive weights is employed, as needed here to process a large-dimensional received data vectors. Although the complexity of the reduced-rank algorithms is higher than that of the full-rank SG-based algorithms, in Section VI we will show that for a limited increase in complexity, they can yield a significant increase in convergence speed and tracking performance when compared to the former, whose performance in the current application is simply unacceptable. In Fig. 2 and Fig. 3, we show the computational complexity against the number of received antenna elements for the recently reported MSER-based reduced-rank algorithms [38], [40] and the proposed MSER-JPDF reduced-rank algorithms. In particular, we consider a commonly used configuration with $P=3$, $I=12$ and $D=10$. From these results, we find that the proposed algorithms have significantly lower complexity than the existing MSER-MSWF reduced-rank algorithm[6] [38]. Although the complexity of the proposed algorithms increases as the number $B$ of branches increases, it remains lower than that of the MSER-JIO reduced-rank algorithms [40] for a large number of antenna elements. Note that for the proposed adaptive MSER-JPDF reduced-rank algorithms with the automatic selection scheme, the numbers of multiplications and additions are the same as those shown in Table III and IV, but with parameters $D_{max}$ and $I_{max}$ instead of $D$ and $I$. In addition, a simple search over the values of $\varepsilon_l^{D,I}(i)$ is performed in order

[6]Note that the MSER-based MSWF reduced-rank algorithm [38] corresponds to the use of the procedure in [15] to construct $\mathbf{S}_D(i)$ and of the MSER-SG adaptive algorithm in [35], [7], to compute $\bar{\mathbf{w}}(i)$.

to select the optimal parameter values $D_{l,opt}$ and $I_{l,opt}$, whose time complexity is about $1.5(D_{max}-D_{min})(I_{max}-I_{min})$. In Section VI, we will show that the estimation and detection performance of the proposed MSER-JPDF exceeds that of existing adaptive reduced-rank algorithms by a wide margin.

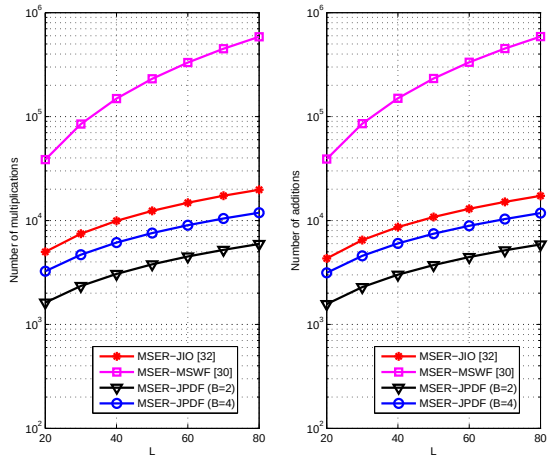


Fig. 2. Comparison of computational complexity for the recently reported reduced-rank algorithms and the proposed MSER-JPDF reduced-rank algorithms in the case of BPSK symbols ($I=12$, $D=10$, $B=2,4$).

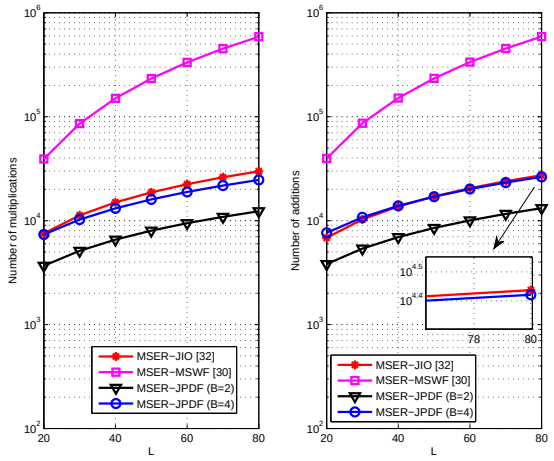


Fig. 3. Comparison of computational complexity for the recently reported reduced-rank algorithms and the proposed MSER-JPDF reduced-rank algorithms in the case of QAM symbols ($I=12$, $D=10$, $B=2,4$).

### *B. Convergence Analysis*

In the following, we discuss the convergence behavior of the proposed algorithms for the joint design of the preprocessing filter and reduced-rank receive filter. Firstly, we focus on the adaptive MSER-JPDF reduced-rank algorithm with BPSK symbols, and provide a proof for its convergence by considering a given branch, i.e., a fixed value of $l \in \{0,1,\ldots,B-1\}$. From [35], [7], we can see that for the average SER cost function $\tilde{\mathcal{P}}_e^l(\bar{\mathbf{w}}_l,\mathbf{p}_l)$ corresponding to the $l$-th branch, by fixing the preprocessor $\mathbf{p}_l$, there will exist infinitely many global MSER solutions for the reduced-rank receive filter $\bar{\mathbf{w}}_l$, which form an infinite half line in the filter weight space[7]. Since the cost function is symmetric in $\bar{\mathbf{w}}_l$ and $\mathbf{p}_l$, similarly by fixing $\bar{\mathbf{w}}_l$, there will be multiple global MSER solutions for $\mathbf{p}_l$. In the proposed SG-based adaptive algorithm, for each branch $l$ at time index $i$, we try to find the gradient direction along the instantaneous SER cost function surface for $\mathbf{p}_l(i)$ and $\bar{\mathbf{w}}_l(i)$, respectively, in order to compute $\mathbf{p}_l(i+1)$ and $\bar{\mathbf{w}}_l(i+1)$. By using small step sizes, $N$ SG iterative steps are approximately equivalent, on average, to a single larger step in the direction of steepest decent on the average SER performance surface $\tilde{\mathcal{P}}_e^l(\bar{\mathbf{w}}_l,\mathbf{p}_l)$, where $N$ is a large integer [11]. Hence, the instantaneous gradient can be replaced by a less noisy average, leading to the following steepest descent update expressions:

$$\mathbf{p}_l((m+1)N)=\mathbf{p}_l(mN)-\alpha_p\frac{\tilde{\mathcal{P}}_e^l(\bar{\mathbf{w}}_l(mN),\mathbf{p}_l(mN))}{\partial\mathbf{p}_l^*} \quad (56)$$

$$\mathbf{w}_l((m+1)N)=\mathbf{w}_l(mN)-\alpha_w\frac{\tilde{\mathcal{P}}_e^l(\bar{\mathbf{w}}_l(mN),\mathbf{p}_l((m+1)N))}{\partial\bar{\mathbf{w}}_l^*} \quad (57)$$

where $m\in\{0,1,2,\ldots\}$ denotes the index of blocks of received vectors, and $\alpha_w$ and $\alpha_p$ are the step sizes for the reduced-rank receive and preprocessing filters, respectively. Therefore, by following (56) and (57) we can obtain the following inequalities for the average SER corresponding to the $l$-th branch:

$$\tilde{\mathcal{P}}_e^l(\mathbf{p}_l((m+1)N),\bar{\mathbf{w}}_l(mN))\le\tilde{\mathcal{P}}_e^l(\mathbf{p}_l(mN),\bar{\mathbf{w}}_l(mN)) \quad (58)$$

and

$$\tilde{\mathcal{P}}_e^l(\mathbf{p}_l((m+1)N),\bar{\mathbf{w}}_l((m+1)N))\le\tilde{\mathcal{P}}_e^l(\mathbf{p}_l((m+1)N),\bar{\mathbf{w}}_l(mN)). \quad (59)$$

This algorithm starts from the initial values $\bar{\mathbf{w}}_l(0)$ and $\mathbf{p}_l(0)$. By using (58) and (59), we obtain

$$\begin{aligned}\ldots&\le\tilde{\mathcal{P}}_e^l(\mathbf{p}_l((m+1)N),\bar{\mathbf{w}}_l((m+1)N))\\&\le\tilde{\mathcal{P}}_e^l(\mathbf{p}_l((m+1)N),\bar{\mathbf{w}}_l(mN))\\&\le\tilde{\mathcal{P}}_e^l(\mathbf{p}_l(mN),\bar{\mathbf{w}}_l(mN))\le\ldots\le\tilde{\mathcal{P}}_e^l(\mathbf{p}_l(N),\bar{\mathbf{w}}_l(N))\\&\le\tilde{\mathcal{P}}_e^l(\mathbf{p}_l(N),\bar{\mathbf{w}}_l(0))\le\tilde{\mathcal{P}}_e^l(\mathbf{p}_l(0),\bar{\mathbf{w}}_l(0)).\end{aligned} \quad (60)$$

This shows that as the number of iterations increases the average SER of each branch $l$ decreases. Therefore, since the SER value is lower bounded by 0, the adaptive MSER-JPDF reduced-rank algorithm for each branch is convergent. Furthermore, at each time index after updating the reduced-rank receive and preprocessing filters for all the branches, we select the optimal branch $l_{opt}$ corresponding to the minimum Euclidean distance between the true transmit symbol and the filter output of each branch (see (13)). By taking the average over independent realizations, we obtain that the average SER of the proposed multiple filtering branches scheme is lower than the average SER of each branch and it decreases with increasing of the number of iterations.

[7]By fixing the preprocessing filter, based on the discussion in [35]-[36], we obtain that any local minimizer of the SER cost function is a global minimizer. Let $\bar{\mathbf{w}}_{l,opt}$ be such a global MSER solution for the $l$-th branch. According to [35] the weight vectors $a\bar{\mathbf{w}}_{l,opt}$, $a>0$, are all global MSER solutions for branch $l$, which form an infinite half line in the filter weight space.

Compared to the proposed algorithm for BPSK symbols in Table I, the proposed algorithm for $M$-QAM symbols in Table II has two extra operations, namely steps 6 and 8. Those operations are carried out after each adaptive iteration to adjust the preprocessing and the reduced-rank receive filters, respectively, in order to guarantee that $\omega_{0,0}$ is positive real as needed for $M$-QAM detection; however, these operations do not affect the convergence. Thus, for each branch we still have $\tilde{\mathcal{P}}_e^l(\mathbf{p}_l((m+1)N), \bar{\mathbf{w}}_l((m+1)N)) \leq \tilde{\mathcal{P}}_e^l(\mathbf{p}_l((m+1)N), \bar{\mathbf{w}}_l(mN)) \leq \tilde{\mathcal{P}}_e^l(\mathbf{p}_l(mN), \bar{\mathbf{w}}_l(mN))$ at the $m$-th block of received vectors. Hence, a similar analysis as above can be done for the adaptive MSER-JPDF reduced-rank algorithm with $M$-QAM symbols, thereby showing the convergence of this algorithm.

## VI. Simulations

In this section, we evaluate the performance of the proposed adaptive MSER-JPDF reduced-rank algorithms and compare them with existing adaptive full-rank and reduced-rank algorithms. Monte-carlo simulations are conducted to verify the effectiveness of the MSER-JPDF adaptive reduced-rank SG algorithms for large-scale multiple-antenna systems. In the simulations, we assume that the base station is equipped with $L = 40$ antenna elements and the system includes one desired user and $K-1$ interfering users. We adopt an observation window of $P = 3$ symbols, the multipath channels (the channel vectors $[h_{k,\nu,0}(i), \ldots, h_{k,\nu,L_p-1}(i)]^T$) are modeled by FIR filters, with the $L_p$ coefficients spaced by one symbol. The channel are time varying over the transmitted symbols, where the profile follows the Universal Mobile Telecommunications System (UMTS) Vehicular A channel model [42] with $L_p = 3$, and the fading is given by Clarke's model [43]. The $K$ users have identical transmit power, which is normalized to unity for convenience. We set $\rho = 1.06\sigma$ [33], [88], [89] in (30), (31), (49) and (50). The full-rank, reduced-rank and preprocessing filters are initialized as $\mathbf{h}_{0,0}(0)$, $\mathbf{T}_l\mathbf{h}_{0,0}(0)$ and $[1, 0, \ldots, 0]^T$ with appropriate dimensions, respectively[8]. The algorithms process 300 symbols in the training mode, which is followed by a decision directed mode of operation.

In the first experiment, we investigate the effects of $D$ and $I$ on the proposed adaptive MSER-JPDF reduced-rank algorithm for BPSK symbols and 16-QAM symbols, respectively. In particular, we consider the case with $B = 4$ branches. In Fig. 4(a) and (b), we show the SER performance of the proposed algorithms (Table I and II) versus $I$ for $D = 6, 8, 10, 12$. The SER is evaluated for data records of 1500 symbols. Note that Fig. 4(a) and (b) correspond to the algorithm with BPSK and 16-QAM symbols, respectively. In order to provide the best performance, we tuned $\mu_w = \mu_p = 0.01$ for Fig. 4(a) and $\mu_w = \mu_p = 0.006$ for Fig. 4(b). For the case with BPSK symbols, we use 10dB for the input SNR while the normalized Doppler frequency is $f_dT_s = 10^{-5}$, where $f_d$ is the Doppler frequency in Hz and $T_s$ is the symbol duration. For the case with 16-QAM symbols, we set SNR= 12dB and $f_dT_s = 10^{-6}$. Notice that we have conducted experiments

[8]The full-rank and reduced-rank receive filters are initialized based on the desired symbol's matched filter, i.e., $\mathbf{h}_{0,0}(0)$. In this work, we assume that this information is known as a priori knowledge for simplicity. In practice, it should be obtained by implementing channel estimation algorithms.

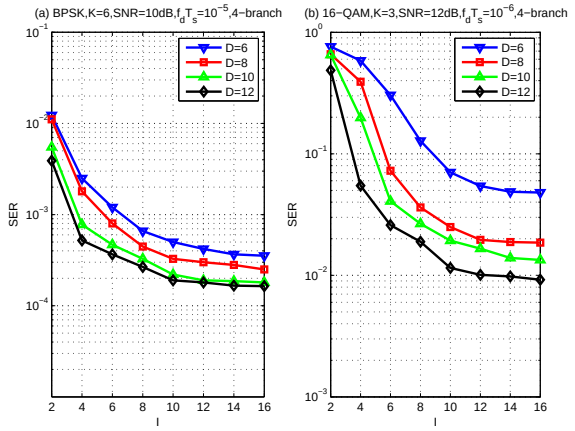


Fig. 4. SER performance versus parameter $I$ with different values of $D$ for the adaptive MSER-JPDF reduced-rank algorithms: (a) BPSK symbols ($K = 6$, SNR $= 10$dB, $f_dT_s = 10^{-5}$); (b) 16-QAM symbols ($K = 3$, SNR $= 12$dB, $f_dT_s = 10^{-6}$).

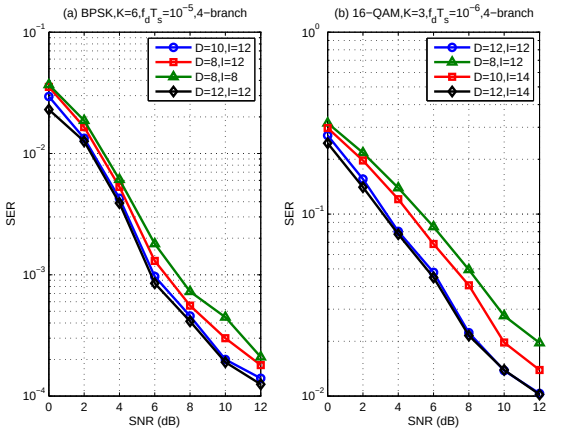


Fig. 5. SER performance of the adaptive MSER-JPDF reduced-rank algorithms versus SNR for different values of $D$ and $I$: (a) BPSK symbols ($K = 6$, $f_dT_s = 10^{-5}$); (b) 16-QAM symbols ($K = 3$, $f_dT_s = 10^{-6}$).

to obtain the most adequate values of parameters $D$ and $I$ for these algorithms and values beyond the range shown here need not be considered since they do not lead to performance improvements. From the results of Fig. 4(a), we can see that the SER initially decreases with an increase of $I$, but beyond $I = 12$ the performance does not change significantly. In order to keep a low complexity we adopt $I = 12$ and $D = 10$ for the proposed algorithm with fixed $D$ and $I$ in the case of BPSK symbols, but also later compare this choice with the proposed algorithm that uses the automatic parameter selection. Similarly, based on the results shown in Fig. 4(b) we select $D = I = 12$ for the proposed algorithm with 16-QAM symbols. Fig. 5(a) and (b) illustrate the SER performance of the adaptive MSER-JPDF reduced-rank algorithms versus SNR for different values of $D$ and $I$, corresponding to the case with BPSK and 16-QAM symbols, respectively. We employ data records of 1500 symbols. The algorithms are run with $B = 4$ branches and the normalized Doppler frequency is set to $f_dT_s = 10^{-6}$. From the results in this figure, we can see that the selected values of $D$ and $I$ offer a good tradeoff between

complexity and performance for the proposed algorithms with fixed $D$ and $I$.

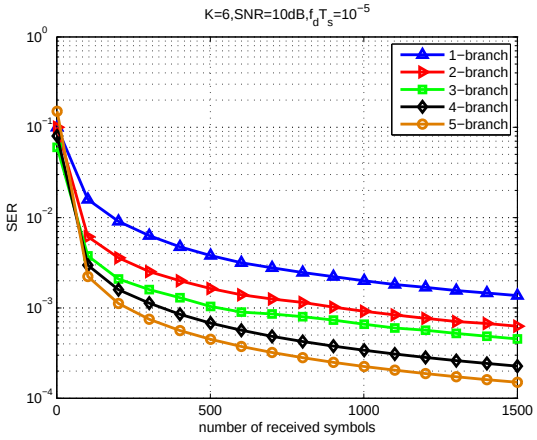


Fig. 6. SER performance of the adaptive MSER-JPDF reduced-rank algorithm with BPSK symbols versus the number of received symbols for different number of branches ($K = 6$, SNR $= 10$dB, $f_dT_s = 10^{-5}$).

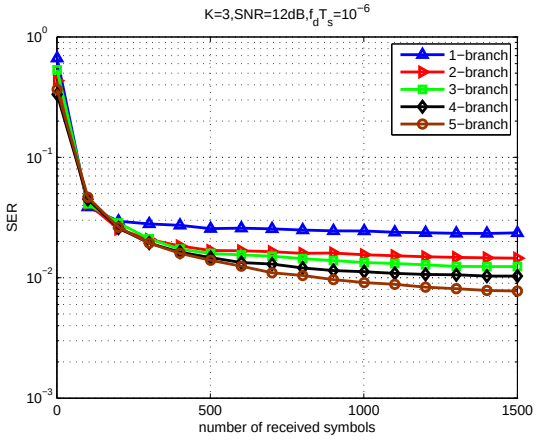


Fig. 7. SER performance of the adaptive MSER-JPDF reduced-rank algorithm with 16-QAM symbols versus the number of received symbols for different number of branches ($K = 3$, SNR $= 12$dB, $f_dT_s = 10^{-6}$).

In the next experiment, we study the impact of the number of branches on the performance of the proposed algorithms. In Fig. 6 and Fig. 7, we study the convergence behavior of the proposed algorithms by showing the evolution of the SER performance as a function of the number of received symbols[9]. We designed the adaptive MSER-JPDF reduced-rank algorithms with $B = 1, 2, 3, 4, 5$ parallel branches. Fig. 6 shows the performance of the BPSK case, where the other system parameters are set as follows: $K = 6$, SNR $= 10$dB and $f_dT_s = 10^{-5}$; while Fig. 7 shows the performance for the 16-QAM case, where the other parameters are: $K = 3$, SNR $= 12$dB and $f_dT_s = 10^{-6}$. The values of step-size are adjusted as in the previous experiment. From these results, it can be noted that the performance of the proposed MSER-JPDF algorithms improves as the number of parallel branches, i.e. parameter $B$, increases. In this regard, we adopt $B = 2$ and $B = 4$ for the remaining experiments because they present an interesting tradeoff between performance and complexity.

[9]The on-line adaptive algorithms update the filters once for each received symbol. The $i$-th symbol time instant corresponds to the $i$-th adaptive iteration, and $T_s$ also corresponds to the time between iterations.

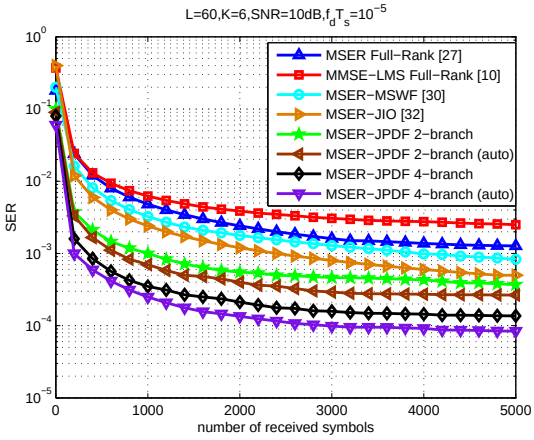


Fig. 8. SER performance of the adaptive MSER-JPDF reduced-rank algorithm with BPSK symbols versus the number of received symbols ($K = 6$, SNR $= 10$dB, $f_dT_s = 10^{-5}$).

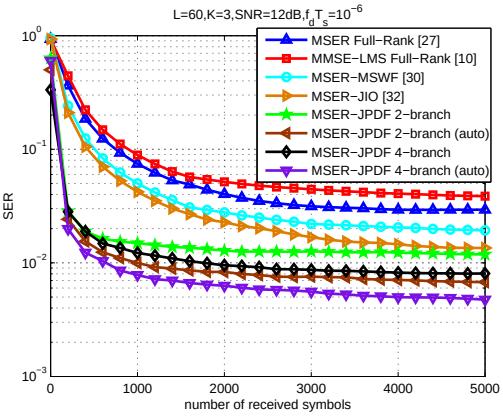


Fig. 9. SER performance of the adaptive MSER-JPDF reduced-rank algorithm with 16-QAM symbols versus the number of received symbols ($K = 3$, SNR $= 12$dB, $f_dT_s = 10^{-6}$).

Fig. 8 and Fig. 9 show the SER performance versus the number of received symbols for the proposed adaptive MSER-JPDF reduced-rank algorithms with fixed and automatic parameter selection schemes and for the existing adaptive full-rank and reduced-rank algorithms, namely: the MSER-SG full-rank adaptive algorithm [7], [35], the MMSE-based LMS full-rank adaptive algorithm [11], the MSER-based MSWF adaptive reduced-rank algorithm [38] and the MSER-based adaptive JIO reduced-rank algorithm [40]. In Fig. 8, we focus on the case of BPSK symbols where the algorithm summarized in Table I is applied. The other system parameters are set to: $K = 6$, SNR $= 10$dB and $f_dT_s = 10^{-5}$. Fig. 9 focuses on the 16-QAM symbols where the algorithm in Table II is applied; the other system parameters are: $K = 3$, SNR $= 12$dB and $f_dT_s = 10^{-6}$. The main algorithm parameters in the experiments are adjusted as given in Table V for the BPSK case and in Table VI for the 16-QAM case. We note that these parameter values for the various algorithms under comparison

have been optimized based on simulations. In order to focus on the main contribution, we only consider the uncoded system in this work. From the results, we can see that the proposed adaptive reduced-rank algorithms with the automatic parameter selection scheme achieve the best convergence performance, followed by the proposed algorithms with fixed values of $D$ and $I$, the recently proposed MSER-JIO adaptive reduced-rank algorithm and the other analyzed algorithms. In our studies, the steady-state SER performance of the proposed reduced-rank algorithms is consistently lower than that of the conventional algorithms. Due to the novel MSER-JPDF scheme, the proposed reduced-rank algorithms outperform the conventional algorithms in terms of both convergence behavior and steady-state performance.

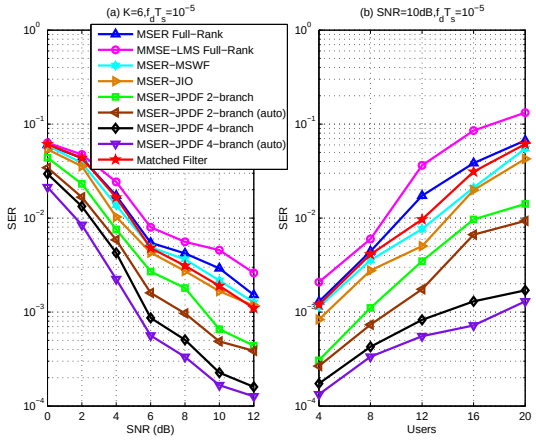


Fig. 10. SER performance for BPSK symbols versus: (a) SNR ($K = 6$); (b) number of users $K$ (SNR $= 10$ dB).

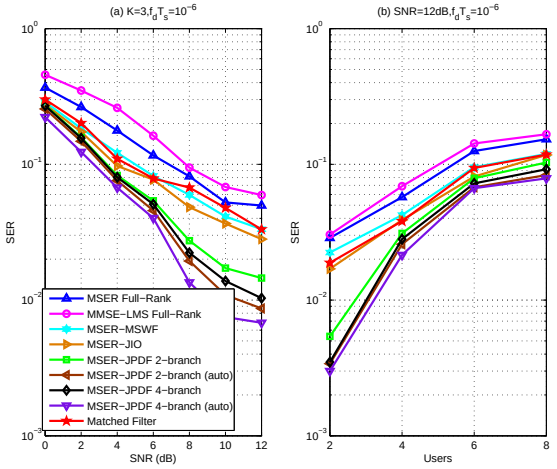


Fig. 11. SER performance for 16-QAM symbols versus: (a) SNR ($K = 3$); (b) number of users $K$ (SNR $= 12$ dB).

Fig. 10(a) and (b) show the SER performance of the desired user versus the SNR and the number of users $K$ for BPSK symbols, respectively, where we set $f_dT_s = 10^{-5}$. The SER is evaluated for data records of $1500$ symbols. Fig. 11(a) and (b) show the corresponding results for 16-QAM symbols, where we set $f_dT_s = 10^{-6}$. The optimized parameter values of the algorithms are shown in Table V and Table VI. From the results, we can see that the best performance is achieved with the proposed adaptive MSER-JPDF reduced-rank algorithms, followed by the adaptive MSER-JIO reduced-rank algorithm, the adaptive MSER-MSWF reduced-rank algorithm, the matched filter, the MSER full-rank adaptive algorithm and the MMSE-based LMS full-rank adaptive algorithm. In particular, for the BPSK case the adaptive MSER-JPDF reduced-rank algorithm with the automatic parameter selection scheme (2 branches) can lead to a $4$dB gain in SNR and support $5$ more users in comparison with the adaptive MSER-MSWF reduced-rank algorithm at the SER level of $10^{-3}$. For the 16-QAM case, the proposed algorithm with the automatic parameter selection scheme (2 branches) can lead to a gain more than $4$dB in SNR and support 2 more users compared to the adaptive MSER-JIO reduced-rank algorithm at the SER level of $2 \times 10^{-2}$.

Furthermore, we consider a measure which relates SER and computational complexity at the same time to compare the proposed reduced-rank algorithms with the conventional reduced-rank algorithms. In this scenario, we compute the packet success probability to computational complexity ratio (PCR), which is expressed as $\frac{(1-SER)^n}{m}$, where $n$ denotes the number of symbols per packet and $m$ denotes the number of computations per packet. For simplicity, we focus on using the number of multiplications as a measure of the computational complexity. Tables VII and VIII show the PCR values versus different values of SNR for BPSK and 16-QAM symbols, respectively, where we set $n = 20$. The system parameters are to those used in Fig. 10(a) and Fig. 11(a). From the results, we can see that the proposed reduced-rank algorithms provide larger PCR values compared to the conventional reduced-rank algorithms, which indicates that the proposed algorithms can improve the performance with reduced computational complexity.

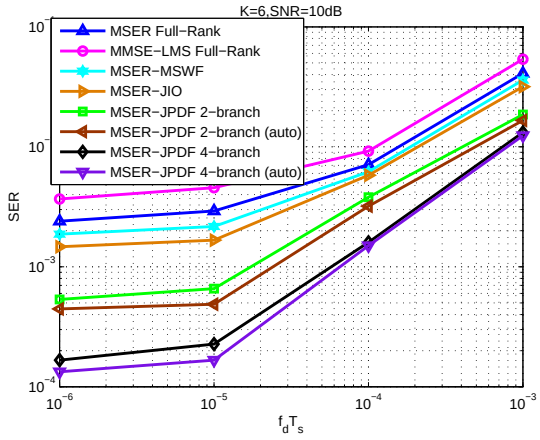


Fig. 12. SER performance versus $f_dT_s$ (cycles/symbol) for BPSK symbols (SNR $= 10$dB, $K = 6$).

In Fig. 12 and Fig. 13, we show the SER performance of the analyzed adaptive algorithms as the fading rate of the channel varies, where we employ data records of $1500$ symbols. The results of Fig. 12 are based on BPSK symbols, where we set $K = 6$ and SNR $= 10$dB, while Fig. 13 focuses on the 16-QAM case, where $K = 3$ and SNR $= 12$dB. The values of algorithm step-sizes used in these experiments are optimized

TABLE V
OPTIMIZED ALGORITHM PARAMETERS FOR BPSK SYMBOLS

| | |
|---|---|
| MMSE-LMS Full-Rank | $\mu_w = 0.015$ |
| MSER Full-Rank | $\mu_w = 0.02$ |
| MSER-MSWF | $\mu_w = 0.05,\ D = 10$ |
| MSER-JIO | $\mu_w = 0.03,\ \mu_S = 0.03,\ D = 10$ |
| MSER-JPDF | $\mu_w = 0.01,\ \mu_p = 0.01,\ D = 10,\ I = 12$ |
| MSER-JPDF (auto) | $\mu_w = \mu_p = 0.006,\ D_{max} = 10,\ D_{min} = 6,\ I_{max} = 12,\ I_{min} = 6$ |

TABLE VI
OPTIMIZED ALGORITHM PARAMETERS FOR 16-QAM SYMBOLS

| | |
|---|---|
| MMSE-LMS Full-Rank | $\mu_w = 0.0015$ |
| MSER Full-Rank | $\mu_w = 0.004$ |
| MSER-MSWF | $\mu_w = 0.03,\ D = 12$ |
| MSER-JIO | $\mu_w = 0.008,\ \mu_S = 0.008,\ D = 12$ |
| MSER-JPDF | $\mu_w = 0.006,\ \mu_p = 0.006,\ D = 12,\ I = 12$ |
| MSER-JPDF (auto) | $\mu_w = \mu_p = 0.003,\ D_{max} = 12,\ D_{min} = 6,\ I_{max} = 12,\ I_{min} = 6$ |

TABLE VII
COMPARISON OF PCR VALUES FOR BPSK SYMBOLS

| Algorithms | SNR = 0dB | SNR = 4dB | SNR = 8dB | SNR = 12dB |
|---|---|---|---|---|
| MSER-JPDF ($B = 2$) | $4.52 \times 10^{-6}$ | $9.54 \times 10^{-6}$ | $1.07 \times 10^{-5}$ | $1.1 \times 10^{-5}$ |
| MSER-JPDF ($B = 4$) | $3.05 \times 10^{-6}$ | $5.1 \times 10^{-6}$ | $5.5 \times 10^{-6}$ | $5.53 \times 10^{-6}$ |
| MSER-MSWF | $4.49 \times 10^{-8}$ | $1.15 \times 10^{-7}$ | $1.4 \times 10^{-7}$ | $1.47 \times 10^{-7}$ |
| MSER-JIO | $1.12 \times 10^{-6}$ | $2.74 \times 10^{-6}$ | $3.19 \times 10^{-6}$ | $3.292 \times 10^{-6}$ |

TABLE VIII
COMPARISON OF PCR VALUES FOR 16-QAM SYMBOLS

| Algorithms | SNR = 0dB | SNR = 4dB | SNR = 8dB | SNR = 12dB |
|---|---|---|---|---|
| MSER-JPDF ($B = 2$) | $9.0 \times 10^{-9}$ | $9.21 \times 10^{-7}$ | $2.98 \times 10^{-6}$ | $3.87 \times 10^{-6}$ |
| MSER-JPDF ($B = 4$) | $5.0 \times 10^{-9}$ | $4.86 \times 10^{-7}$ | $1.65 \times 10^{-6}$ | $2.11 \times 10^{-6}$ |
| MSER-MSWF | $1.4 \times 10^{-10}$ | $9.37 \times 10^{-9}$ | $3.67 \times 10^{-8}$ | $6.35 \times 10^{-8}$ |
| MSER-JIO | $3.0 \times 10^{-9}$ | $2.88 \times 10^{-7}$ | $8.27 \times 10^{-7}$ | $1.26 \times 10^{-6}$ |

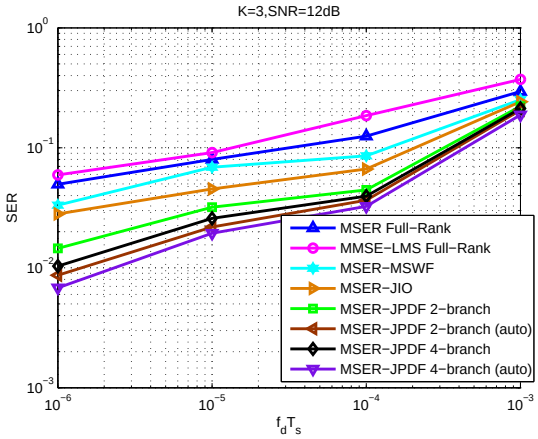


Fig. 13. SER performance versus $f_dT_s$ (cycles/symbol) for 16-QAM symbols (SNR = 12dB, $K = 3$).

for each value of $f_dT_s$. In particular, for the proposed algorithms with BPSK, we use $\mu_w = \mu_p = 0.01, 0.01, 0.005, 0.002$ for $f_dT_s = 10^{-6}, 10^{-5}, 10^{-4}, 10^{-3}$, respectively; for the 16-QAM case, we use $\mu_w = \mu_p = 0.006, 0.001, 0.0005, 0.0005$ for $f_dT_s = 10^{-6}, 10^{-5}, 10^{-4}, 10^{-3}$, respectively. First, we can see that as the fading rate increases, the performance becomes worse, although our proposed algorithms outperform the existing algorithms. Moreover, we observe that the proposed algorithms with 4 branches perform better than in the case with 2 branches. Fig. 12 and Fig. 13 show the ability of the adaptive MSER-JPDF reduced-rank algorithms to deal with channel variations for both BPSK and QAM symbols. Despite their low complexity, the full-rank SG-based algorithms can only achieve a poor performance, inadequate for practical applications. The SER performance of the analyzed adaptive algorithms in Fig. 13 is not as good as in Fig. 12, since detecting a high order modulation symbol is harder than detecting a low order modulation symbol, specially for large values of $f_dT_s$.

## VII. CONCLUSION

In this paper, we have proposed an adaptive JPDF reduced-rank strategy based on the MSER criterion for the design of a receive-processing front-end in multiuser large-scale multiple-antenna systems. The proposed scheme employs a multiple-branch processing structure which adaptively performs dimensionality reduction using a set of jointly optimized preprocessing and decimation units, followed by receive filtering. The final decision is switched to the branch with the best performance based on the minimum Euclidean distance during a training period. We have developed SG based algorithms for the adaptive implementation of the preprocessing filter and the reduced-rank receive filter in the case of BPSK and QAM symbols. An automatic parameter selection scheme has been proposed to determine the lengths of the preprocessor and the reduced-rank receive filter during their operation. We

focused on the computational complexity and convergence to perform the analysis of the proposed algorithms. The results have shown that the proposed scheme significantly outperforms existing reduced-rank algorithms and can support communication systems with higher loads, i.e. larger number of mobile users for a given quality of services. Future work will consider nonlinear detectors and other multiple-antenna configurations [44]-[87].

## REFERENCES


[1] T. L. Marzetta, "Noncooperative cellular wireless with unlimited numbers of base station antennas," *IEEE Trans. Wireless Commun.*, vol. 9, no. 11, pp. 3590-3600, Nov. 2010.

[2] P. Li and R.D. Murch, "Multiple output selection-LAS algorithm in large MIMO systems," *IEEE Commun. Lett.*, vol.14, no.5, pp. 399-401, May 2010.

[3] R. C. de Lamare, "Massive MIMO Systems: Signal Processing Challenges and Future Trends," *URSI Radio Science Bulletin*, 2013.

[4] S. K. Mohammed, A., A. Chockalingam, and B. S. Rajan, "High rate space-time coded large-MIMO systems: Low-complexity detection and channel estimation", *IEEE Journal Sel. Topics Signal Process.*, vol. 3, no. 6, pp. 958-974, Dec. 2009.

[5] J. Arnau, B. Devillers, C. Mosquera, and A. Pérez-Neira, "Performance study of multiuser interference mitigation schemes for hybrid broadband multibeam satellite architectures", *EURASIP J. on Wireless Commun. and Networking*, 2012:132, Apr. 2012.

[6] W. Zhang, H. Ren, C. Pan, M. Chen, R. C. de Lamare, B. Du and J. Dai, "Large-Scale Antenna Systems With UL/DL Hardware Mismatch: Achievable Rates Analysis and Calibration", IEEE Trans. Commun., vol.63, no.4, pp. 1216-1229, April 2015.

[7] S. Chen, A. Livingstone, H.-Q. Du, and L. Hanzo, "Adaptive minimum symbol error rate beamforming assisted detection for quadrature amplitude modulation," *IEEE Trans. Wireless Commun.*, vol. 7, no. 4, pp. 1140-1145, Apr. 2008.

[8] D. H. Johnson and D. E. Dudgeon, *Array Signal Processing: Concepts and Techniques*, Englewood Cliffs, NJ: Prentice-Hall, 1993.

[9] S. Anderson, M. Millnert, M. Viberg, and B. Wahlberg, "An adaptive array for mobile communication systems," *IEEE Trans. Vehi. Technol.*, vol. 40, no. 1, pp. 230-236, Feb. 1991.

[10] F. Rusek, D. Persson, B. K. Lau, E. G. Larsson, T. L. Marzetta, O. Edfors, and F. Tufvesson, "Scaling up MIMO: opportunities and challenges with very large arrays," *IEEE Signal Process. Mag.*, vol. 30, no. 1, pp. 40-60, Jan. 2013.

[11] S. Haykin, *Adaptive Filter Theory*, 4th ed. Englewood Cliffs, NJ: Prentice-Hall, 2002.

[12] A. M. Haimovich and Y. Bar-Ness, "An eigenanalysis interference canceler," *IEEE Trans. Signal Process.*, vol. 39, no. 1, pp. 76-84, Jan. 1991.

[13] J. S. Goldstein and I. S. Reed, "Reduced-rank adaptive filtering," *IEEE Trans. Signal Process.*, vol. 45, no. 2, pp. 492-496, Feb. 1997.

[14] J. S. Goldstein, I. S. Reed, and L. L. Scharf, "A multistage representation of the Wiener filter based on orthogonal projections," *IEEE Trans. Inf. Theory*, vol. 44, no. 11, pp. 2943-2959, Nov. 1998.

[15] M. L. Honig and J. S. Goldstein, "Adaptive reduced-rank interference suppression based on the multistage Wiener filter," *IEEE Trans. Commun.*, vol. 50, no. 6, pp. 986-994, Jun. 2002.

[16] L.-L. Yang, "Capacity and error performance of reduced-rank transmitter multiuser preprocessing based on minimum power distortionless response," *IEEE Trans. Wireless Commun.*, vol.7, no.11, pp. 4646-4655, Nov. 2008.

[17] R. C. de Lamare and Raimundo Sampaio-Neto, "Reduced-rank Interference Suppression for DS-CDMA based on Interpolated FIR Filters", *IEEE Communications Letters*, vol. 9, no. 3, March 2005.

[18] R. C. de Lamare and R. Sampaio-Neto, "Adaptive Reduced-Rank MMSE Filtering with Interpolated FIR Filters and Adaptive Interpolators", *IEEE Signal Processing Letters*, vol. 12, no. 3, March, 2005.

[19] R. C. de Lamare and R. Sampaio-Neto, "Adaptive Interference Suppression for DS-CDMA Systems based on Interpolated FIR Filters with Adaptive Interpolators in Multipath Channels", *IEEE Trans. Vehicular Technology*, Vol. 56, no. 6, September 2007.

[20] R. C. de Lamare, "Adaptive Reduced-Rank LCMV Beamforming Algorithms Based on Joint Iterative Optimisation of Filters," Electronics Letters, 2008.

[21] R. C. de Lamare and R. Sampaio-Neto, "Reduced-rank adaptive filtering based on joint iterative optimization of adaptive filters", *IEEE Signal Process. Lett.*, vol. 14, no. 12, pp. 980-983, Dec. 2007.

[22] R. C. de Lamare, M. Haardt, and R. Sampaio-Neto, "Blind Adaptive Constrained Reduced-Rank Parameter Estimation based on Constant Modulus Design for CDMA Interference Suppression", *IEEE Transactions on Signal Processing*, June 2008.

[23] R. C. de Lamare and R. Sampaio-Neto, "Reduced-rank space-time adaptive interference suppression with joint iterative least squares algorithms for spread-spectrum systems," *IEEE Trans. Vehi. Technol.*, vol. 59, no. 3, pp. 1217-1228, Mar. 2010.

[24] R. C. de Lamare and R. Sampaio-Neto, "Adaptive reduced-rank equalization algorithms based on alternating optimization design techniques for MIMO systems," *IEEE Trans. Vehi. Technol.*, vol. 60, no. 6, pp. 2482-2494, Jul. 2011.

[25] R. Fa and R. C. de Lamare, "Reduced-rank STAP algorithms using joint iterative optimization of filters," *IEEE Trans. Aerosp. Electron. Syst.*, vol. 47, no. 3, pp. 1668-1684, Jul. 2011.

[26] R. C. de Lamare, L. Wang and R. Fa, "Adaptive reduced-rank LCMV beamforming algorithms based on joint iterative optimization of filters: design and analysis," *Signal Process.*, vol. 90, no. 2, pp. 640-652, Feb. 2010.

[27] R. C. de Lamare, R. Sampaio-Neto and M. Haardt, "Blind adaptive constrained constant-modulus reduced-rank interference suppression algorithms based on interpolation and switched decimation," *IEEE Trans. Signal Process.*, vol. 59, no. 2, pp. 681-695, Feb. 2011.

[28] R. C. de Lamare and R. Sampaio-Neto, "Adaptive Reduced-Rank Processing Based on Joint and Iterative Interpolation, Decimation, and Filtering," *IEEE Trans. Signal Process.*, vol. 57, no. 7, pp. 2503-2514, Jul. 2009.

[29] R.C. de Lamare, R. Sampaio-Neto and M. Haardt, "Blind Adaptive Constrained Constant-Modulus Reduced-Rank Interference Suppression Algorithms Based on Interpolation and Switched Decimation," *IEEE Trans. on Signal Processing*, vol.59, no.2, pp.681-695, Feb. 2011.

[30] S. Li, R. C. de Lamare and R. Fa, "Reduced-Rank Linear Interference Supression for DS-UWB Systems Based on Switched Approximations of Adaptive Basis Functions", *IEEE Transactions on Vehicular Technology*, vol. 60, no. 2, February 2011.

[31] R. C. de Lamare and R. Sampaio-Neto, "Adaptive space-time reduced-rank estimation based on diversity-combined decimation and interpolation applied to interference suppression in CDMA systems," *IET Signal Process.*, vol. 3, no. 2, pp. 150-163, Mar. 2009.

[32] R. C. de Lamare and R. Sampaio-Neto, "Adaptive reduced-rank MMSE filtering with interpolated FIR filters and adaptive interpolators," *IEEE Signal Process. Lett.*, vol. 12, no. 3, Mar. 2005, pp. 177-180.

[33] S. Chen, A. K. Samingan, B. Mulgrew, and L. Hanzo, "Adaptive minimum-BER linear multiuser detection for DS-CDMA signals in multipath channels", *IEEE Trans. Signal Process.*, vol. 49, no. 6, pp. 1240-1247, Jun. 2001.

[34] S. Chen, L. Hanzo, and B. Mulgrew, "Adaptive minimum symbol-error-rate decision feedback equalization for multilevel pulse-amplitude modulation," *IEEE Trans. Signal Process.*, vol. 52, no. 7, pp. 2092-2101, Jul. 2004.

[35] S. Chen, S. Tan, L. Xu, and L. Hanzo, "Adaptive minimum error-rate filtering design: A review," *Signal Process.*, vol. 88, no. 7, pp. 1671-1697, Jul. 2008.

[36] X. F. Wang, W.-S. Lu, A. Antoniou, "Constrained minimum-BER multiuser detection," *IEEE Trans. Signal Process.*, vol. 48, no. 10, pp. 2903-2909, Oct. 2000.

[37] R. C. de Lamare and R. Sampaio-Neto, "Adaptive MBER decision feedback multiuser receivers in frequency selective fading channels", *IEEE Commun. Lett.*, vol. 7, no. 2, pp. 73-75, Feb. 2003.

[38] Q. Z. Ahmed, L-L. Yang, and S. Chen, "Reduced-rank adaptive least bit-error-rate detection in hybrid direct-sequence time-hopping ultrawide bandwidth systems," *IEEE Trans. Vehi. Technol.* vol. 60, no. 3, pp. 849-857, Mar. 2011.

[39] L. D'Orazio, C. Sacchi, M. Donelli, J. Louveaux, and L. Vandendorpe, "A near-optimum multiuser receiver for STBC MC-CDMA systems based on minimum conditional BER criterion and genetic algorithm-assisted channel estimation," *EURASIP J. on Wireless Commun. and Networking*, vol. 2011, Article ID 351494, Mar. 2011, pp. 1-12.

[40] Y. Cai and R. C. de Lamare, "Adaptive linear minimum BER reduced-rank interference suppression algorithms based on joint and iterative optimization of filters", *IEEE Commun. Lett.*, vol. 17, no. 4, pp. 633-636, Apr. 2013.

[41] G. H. Golub and C. F. van Loan, *Matrix Computations*. New York: Wiley, 2002.

[42] Third Generation Partnership Project (3GPP), Specs. 25.101, 25.211-25.215, ver. 5.x.x.

[43] T. S. Rappaport, *Wireless Communications*. Englewood Cliffs, NJ: Prentice-Hall, 1996.

[44] G. D. Golden, C. J. Foschini, R. A. Valenzuela and P. W. Wolniansky, "Detection algorithm and initial laboratory results using V-BLAST space-time communication architecture", *Electronics Letters*, vol. 35, No.1, January 1999.

[45] J. Benesty, Y. Huang, and J. Chen, A fast recursive algorithm for optimum sequential signal detection in a BLAST system, IEEE Trans. Signal Processing, vol. 51, pp. 17221730, July 2003.

[46] A. Rontogiannis, V. Kekatos, and K. Berberidis," A Square-Root Adaptive V-BLAST Algorithm for Fast Time-Varying MIMO Channels," *IEEE Signal Processing Letters*, Vol. 13, No. 5, pp. 265-268, May 2006.

[47] R. Fa, R. C. de Lamare, "Multi-Branch Successive Interference Cancellation for MIMO Spatial Multiplexing Systems", *IET Communications*, vol. 5, no. 4, pp. 484 - 494, March 2011.

[48] P. Li, R. C. de Lamare and R. Fa, "Multiple Feedback Successive Interference Cancellation Detection for Multiuser MIMO Systems," *IEEE Transactions on Wireless Communications*, vol. 10, no. 8, pp. 2434 - 2439, August 2011.

[49] J. H. Choi, H. Y. Yu, Y. H. Lee, Adaptive MIMO decision feedback equalization for receivers with time-varying channels, *IEEE Trans. Signal Proc.*, 2005, 53, no. 11, pp. 4295-4303.

[50] C. Windpassinger, L. Lampe, R.F.H. Fischer, T.A Hehn, "A performance study of MIMO detectors," *IEEE Transactions on Wireless Communications*, vol. 5, no. 8, August 2006, pp. 2004-2008.

[51] Y. H. Gan, C. Ling, and W. H. Mow, Complex lattice reduction algorithm for low-complexity full-diversity MIMO detection, *IEEE Trans. Signal Processing*, vol. 56, no. 7, July 2009.

[52] K. J. Kim, J. Yue, R. A. Iltis, and J. D. Gibson, "A QRD-M/Kalman filter-based detection and channel estimation algorithm for MIMO-OFDM systems", *IEEE Trans. Wireless Communications*, vol. 4,pp. 710-721, March 2005.

[53] Y. Jia, C. M. Vithanage, C. Andrieu, and R. J. Piechocki, Probabilistic data association for symbol detection in MIMO systems, *Electron. Lett.*, vol. 42, no. 1, pp. 3840, Jan. 2006.

[54] S. Yang, T. Lv, R. Maunder, and L. Hanzo, "Unified Bit-Based Probabilistic Data Association Aided MIMO Detection for High-Order QAM Constellations", *IEEE Transactions on Vehicular Technology*, vol. 60, no. 3, pp. 981-991, 2011.

[55] M. K. Varanasi, "Decision feedback multiuser detection: A systematic approach," *IEEE Trans. on Inf. Theory*, vol. 45, pp. 219-240, January 1999.

[56] J. F. Rler and J. B. Huber, "Iterative soft decision interference cancellation receivers for DS-CDMA downlink employing 4QAM and 16QAM," *in Proc. 36th Asilomar Conf. Signal, Systems and Computers*, Pacific Grove, CA, Nov. 2002.

[57] J. Luo, K. R. Pattipati, P. K. Willet and F. Hasegawa, "Optimal User Ordering and Time Labeling for Ideal Decision Feedback Detection in Asynchronous CDMA", *IEEE Trans. on Communications*, vol. 51, no. 11, November, 2003.

[58] G. Woodward, R. Ratasuk, M. L. Honig and P. Rapajic, "Minimum Mean-Squared Error Multiuser Decision-Feedback Detectors for DS-CDMA," *IEEE Trans. on Communications*, vol. 50, no. 12, December, 2002.

[59] R.C. de Lamare, R. Sampaio-Neto, "Adaptive MBER decision feedback multiuser receivers in frequency selective fading channels", *IEEE Communications Letters*, vol. 7, no. 2, Feb. 2003, pp. 73 - 75.

[60] F. Cao, J. Li, and J. Yang, "On the relation between PDA and MMSE-ISDIC," *IEEE Signal Processing Letters*, vol. 14, no. 9, Sep. 2007.

[61] Y. Cai and R. C. de Lamare, "Adaptive Space-Time Decision Feedback Detectors with Multiple Feedback Cancellation", *IEEE Transactions on Vehicular Technology*, vol. 58, no. 8, October 2009, pp. 4129 - 4140.

[62] P. Li and R. C. de Lamare, "Adaptive Decision-Feedback Detection With Constellation Constraints for MIMO Systems", *IEEE Transactions on Vehicular Technology*, vol. 61, no. 2, 853-859, 2012.

[63] M. Reuter, J.C. Allen, J. R. Zeidler, R. C. North, "Mitigating error propagation effects in a decision feedback equalizer", *IEEE Transactions on Communications*, vol. 49, no. 11, November 2001, pp. 2028 - 2041.

[64] R.C. de Lamare, R. Sampaio-Neto, A. Hjorungnes, "Joint iterative interference cancellation and parameter estimation for cdma systems", *IEEE Communications Letters*, vol. 11, no. 12, December 2007, pp. 916 - 918.

[65] K. Vardhan, S. Mohammed, A. Chockalingam and B. Rajan, "A low-complexity dector for large MIMO systems and multicarrier CDMA systems", IEEE J. Sel. Commun., vol. 26, no. 3, pp. 473-485, Apr. 2008.

[66] R.C. de Lamare, R. Sampaio-Neto, Minimum mean-squared error iterative successive parallel arbitrated decision feedback detectors for DS-CDMA systems, IEEE Trans. Commun., vol. 56, no. 5, May 2008, pp. 778-789.

[67] R. C. de Lamare, "Adaptive and Iterative Multi-Branch MMSE Decision Feedback Detection Algorithms for Multi-Antenna Systems", *IEEE Transactions on Wireless Communications*, vol. 14, no. 2, February 2013.

[68] K. Zu and R. C. de Lamare, "Low-complexity lattice reduction-aided regularized block diagonalization for MU-MIMO systems," *IEEE Communication Letters*, vol. 16, no. 6, Jun. 2012.

[69] K. Zu, R. C. de Lamare and M. Haardt, "Generalized design of low-complexity block diagonalization type precoding algorithms for multiuser MIMO systems", IEEE Trans. Communications, 2013.

[70] C. Windpassinger, R. Fischer, T. Vencel and J. Huber, "Precoding in multiantenna and multiuser communications," IEEE Trans. Wireless Commun., vol. 3, no. 4, Jul. 2004.

[71] C.B. Peel, B.M. Hochwald, and A.L. Swindlehurst, A vector-perturbation technique for near capacity multiantenna multiuser communicationpart I: channel inversion and regularization, IEEE Trans. Commun., vol. 53, no. 1, pp. 195202, Jan. 2005.

[72] H. Wymeersch, F. Penna and V. Savic, "Uniformly Reweighted Belief Propagation for Estimation and Detection in Wireless Networks," IEEE Trans. Wireless Communications, vol. PP, No. 99, pp. 1-9, Feb. 2012.

[73] J. Liu, R. C. de Lamare, "Low-Latency Reweighted Belief Propagation Decoding for LDPC Codes," IEEE Communications Letters, vol. 16, no. 10, pp. 1660-1663, October 2012.

[74] A. G. D. Uchoa, C. T. Healy and R. C. de Lamare , "Structured Root-Check LDPC Codes and PEG-Based Techniques for Block-Fading Channels, EURASIP Journal on Wireless Communications and Networking, 2015.

[75] J. Li and R. C. de Lamare, "Low-Latency Reweighted Belief Propagation Decoding for LDPC Codes", *IEEE Communications Letters*, vol. 16, no. 10, October 2012, pp. 1660 - 1663.

[76] A. G. D. Uchoa, C. T. Healy and R. C. de Lamare, "Iterative Detection and Decoding Algorithms For MIMO Systems in Block-Fading Channels using LDPC Codes, IEEE Transactions on Vehicular Technology, 2015.

[77] A. Hakkarainen, J. Werner, K. R. Dandekar and M. Valkama, "Widely-linear beamforming and RF impairment suppression in massive antenna arrays," Journal of Communications and Networks, vol.15, no.4, pp.383,397, Aug. 2013

[78] P. Clarke ad R. C. de Lamare, "Transmit Diversity and Relay Selection Algorithms for Multi-relay Cooperative MIMO Systems", IEEE Transactions on Vehicular Technology, vol. 61 , no. 3, March 2012, Page(s): 1084 - 1098.

[79] T. Adali, P. J. Schreier and L. L. Scharf, "Complex-valued signal processing: the proper way to deal with impropriety", IEEE Trans. Signal Processing, vol. 59, no. 11, pp. 51015125 , November 2011.

[80] N. Song, R. C. de Lamare, M. Haardt, and M. Wolf, "Adaptive Widely Linear Reduced-Rank Interference Suppression based on the Multi-Stage Wiener Filter," IEEE Transactions on Signal Processing, vol. 60, no. 8, 2012.

[81] N. Song, W. U. Alokozai, R. C. de Lamare and M. Haardt, "Adaptive Widely Linear Reduced-Rank Beamforming Based on Joint Iterative Optimization," IEEE Signal Processing Letters, vol.21, no.3, pp. 265-269, March 2014.

[82] R. C. de Lamare and R. Sampaio-Neto, "Sparsity-Aware Adaptive Algorithms Based on Alternating Optimization and Shrinkage," IEEE Signal Processing Letters, vol.21, no.2, pp.225,229, Feb. 2014.

[83] H. Ruan and R. C. de Lamare, "Robust Adaptive Beamforming Using a Low-Complexity Shrinkage-Based Mismatch Estimation Algorithm," IEEE Signal Processing Letters, vol.21, no.1, pp.60,64, Jan. 2014.

[84] H. Harashima and H. Miyakawa, "Matched-transmission technique for channels with intersymbol interference," *IEEE Trans. Commun.*, vol. 20, Aug. 1972.

[85] K. Zu, R. C. de Lamare and M. Haardt, "Multi-Branch Tomlinson-Harashima Precoding Design for MU-MIMO Systems: Theory and Algorithms," IEEE Transactions on Communications, vol.62, no.3, pp.939,951, March 2014.

[86] L. Zhang, Y. Cai, R. C. de Lamare and M. Zhao, "Robust Multibranch TomlinsonHarashima Precoding Design in Amplify-and-Forward MIMO Relay Systems," IEEE Transactions on Communications, vol.62, no.10, pp.3476,3490, Oct. 2014.

[87] Q. Zhou and X. Ma, Element-Based Lattice Reduction Algorithms for Large MIMO Detection, IEEE J. Sel. Areas Commun, vol. 31, no. 2, pp. 274-286, Feb. 2013.

[88] B. W. Silverman, *Density Estimation*, London, U.K.: Chapman and Hall, 1996.

[89] E. Parzen, "On estimation of a probability density function and mode", *Ann. Math. Statist.*, vol. 33, no. 3, pp. 1065-1076, 1962.